Report No. DOE/JPL-954328-79/11
Distribution Category UC-63
JPL Contract No. 954328

QUARTERLY REPORT

DEVELOPMENT OF AN ACCELERATED TEST DESIGN FOR PREDICTING THE SERVICE LIFE OF THE SOLAR ARRAY AT MEAD, NEBRASKA

to

JET PROPULSION LABORATORY
CALIFORNIA INSTITUTE OF TECHNOLOGY

for the

ENCAPSULATION TASK OF THE
LOW-COST SOLAR ARRAY PROJECT

The JPL Low-Cost Solar Array Project is sponsored by the U.S. Department of Energy and forms part of the Solar Photovoltaic Conversion Program to initiate a major effort toward the development of low-cost solar arrays. This work was performed for the Jet Propulsion Laboratory, California Institute of Technology by agreement between NASA and DOE.

February 6, 1979

G. B. Gaines, R. E. Thomas, G. T. Noel,
T. S. Shilliday, V. E. Wood, and D. C. Carmichael

(NASA-CR-158373) DEVELOPMENT OF AN ACCELERATED TEST DESIGN FOR PREDICTING THE SERVICE LIFE OF THE SOLAR ARRAY AT MEAD, NEBRASKA Quarterly Report (Battelle Columbus Labs., Ohio.) 51 p HC A04/MF A01 G3/44 N79-21546 Unclas 16680

BATTELLE
Columbus Laboratories
505 King Avenue
Columbus, Ohio 43201

Report No. DOE/JPL-954328-79/11
Distribution Category UC-63
JPL Contract No. 954328

QUARTERLY REPORT

DEVELOPMENT OF AN ACCELERATED TEST DESIGN FOR PREDICTING THE SERVICE LIFE OF THE SOLAR ARRAY AT MEAD, NEBRASKA

to

JET PROPULSION LABORATORY
CALIFORNIA INSTITUTE OF TECHNOLOGY

for the

ENCAPSULATION TASK OF THE
LOW-COST SOLAR ARRAY PROJECT

The JPL Low-Cost Solar Array Project is sponsored by the U.S. Department of Energy and forms part of the Solar Photovoltaic Conversion Program to initiate a major effort toward the development of low-cost solar arrays. This work was performed for the Jet Propulsion Laboratory, California Institute of Technology by agreement between NASA and DOE.

February 6, 1979

G. B. Gaines, R. E. Thomas, G. T. Noel,
T. S. Shilliday, V. E. Wood, and D. C. Carmichael

BATTELLE
Columbus Laboratories
505 King Avenue
Columbus, Ohio 43201

DEVELOPMENT OF AN ACCELERATED TEST DESIGN FOR PREDICTING THE SERVICE LIFE OF THE SOLAR ARRAY AT MEAD, NEBRASKA

ABSTRACT

Economic viability requires that photovoltaic arrays should have a service life of 20 years or longer. Qualification and performance tests indicate that presently available photovoltaic modules provide acceptable performance at the time of installation. A major question remains as to how long these modules, and lower cost developmental modules, will continue to provide an acceptable level of power in normal environments found in the United States. Determining service life under normal environments (normal levels of environmental "stresses") requires an unacceptable length of time for testing. Therefore, tests which accelerate module aging, without changing the failure mode that occurs under normal stresses, are required to shorten the test period. This study is being conducted as part of a program to develop and validate an accelerated test plan that can be used to predict the useful service life of present and future solar arrays.

Owing to the complexity of a photovoltaic module and the many environmental stresses which can cause power degradation, a complete factorial test program would require too many experiments and be too expensive to be a practical approach to life prediction. In a previous study under this contract (Report No. ERDA/JPL-954328-77/1), a methodology was developed for designing an accelerated test program incorporating trade-offs between the cost of each test and its value in reducing the variance in the life prediction for that array. The objective of the present study is to apply this methodology to develop an accelerated test plan to predict the service life of the 25-kW photovoltaic array installed near Mead, Nebraska.

Potential long-term degradation modes for the two types of modules in the Mead array have been determined and judgments have been made as to those environmental stresses and combinations of stresses which accelerate the degradation of the power output. "Hierarchical trees" representing the severity of effects of stresses (test conditions) on eleven individual degradation modes have been constructed and have been pruned of tests judged to be non-essential. Composites of those trees have been developed so that there is now one pruned tree covering eight degradation modes, another covering two degradation modes, and a third covering one degradation mode. These three composite trees form the basis for selection of test conditions in the final test plan which is now being prepared.

ACKNOWLEDGMENTS

Hugh Maxwell of the Jet Propulsion Laboratory is the Technical Manager for this study and Cliff Coulbert of JPL is the Manager of the Encapsulation Task of the Low-Cost Solar Array (LSA) Project for which this study was performed. Their helpful guidance and technical input to the study are gratefully acknowledged. Information from numerous other JPL staff members associated with the LSA Project has also been helpful in the study.

The authors also wish to express their appreciation for the cooperation and participation of Dr. Marvin Pope, Steve Forman, Ed Murphy, and others of MIT-Lincoln Laboratory which installed and is responsible for the operation of the photovoltaic array near Mead, Nebraska, for the Department of Energy. Information from A. F. Forestieri and others of NASA-Lewis Research Center is also acknowledged.

TABLE OF CONTENTS

LIST OF TABLES

LIST OF FIGURES

DEVELOPMENT OF AN ACCELERATED TEST DESIGN FOR PREDICTING THE SERVICE LIFE OF THE SOLAR ARRAY AT MEAD, NEBRASKA

INTRODUCTION

Economic viability requires that the service life of photovoltaic arrays be approximately 20 years or longer. Qualification and performance tests indicate that presently available arrays and the modules making them up provide acceptable performance at the time of installation. A major question remains as to how long such arrays will continue to provide acceptable power in normal environments found in the United States. Determining service life under normal environments (normal levels of environmental "stresses") requires an unacceptable length of time for testing. Therefore, tests which accelerate module aging, without changing the mode of aging that occurs under normal stresses, are required to compress the test period.

Owing to the complexity of a module and the many environmental stresses which can cause power degradation, a complete-factorial, accelerated test program would require too many experiments and be too expensive to be a practical solution to life prediction. In Study 4 of this contract (Report No. ERDA/JPL-954328-77/1, "Methodology for Designing Accelerated Aging Tests for Predicting Life of Photovoltaic Arrays"), a methodology was developed for designing an accelerated test program incorporating trade-offs between the costs of each test and its value in reducing the variance in the life prediction for that array.(1)

Several features and defined directions of the approach to life predictions impact the program in important ways. Among these features and directions are the following:

1. The primary emphasis is on long-term degradation phenomena at the modular level. This emphasis assumes a mature module design; that is, the infant mortality rate is small. Concomitantly, the emphasis dictates that measurements which are precursors of failure be considered over a count of actual failures.

2. The dependent variable is power output. Ultimately all measurable degradations of module components must be related to this variable. This is a difficult problem. To help mitigate this problem, the test design will include teardown analyses in which more appropriate property changes can be measured in the laboratory.

3. The experimental test design deals with the modules employed in the Mead, Nebraska array, that is, Block II Modules fabricated by two manufacturers: Solerex and Sensor Technology. Additionally, Mead, Nebraska, will represent the normal stress environment.

4. Failures to date have been of the immature-design type. This circumstance means that the dominant long-term failure mode is yet to be identified. A consequence is that the test design must accommodate a best-estimate of several possible failure modes and thus include many stresses and multiple stress levels.

5. Because of the necessary multiple stresses and levels, considerable emphasis in the test design must be placed on separating out of the interactive-stress-test design those degradation phenomena which can be treated as independent tests, so as to keep the cost of the total test design to an acceptable level. For example, dirt and hail effects can probably be treated in such a manner.

The developed methodology, as delineated in the previously referenced Study 4 Report(1), encompasses 22 steps leading to the final test design. The work on this study has been directed to the application of these steps to the specific array already installed at Mead, Nebraska. It has progressed to the point of identifying for separate treatment, those stresses which would create intolerable technical or economic problems if accommodated simultaneously with all of the other stresses. Further, "hierarchical trees" representing the effects of stresses (test conditions) on elevan individual degradation modes have been constructed and then pruned of tests judged to be nonessential. Composites of those trees have been developed so that there is now one pruned tree covering eight degradation modes, another covering two degradation modes, and a third covering one degradation mode. These three composite trees are represented in the form of the final test plan which is now being prepared.

OBJECTIVES

As a significant beginning in applying accelerated tests to solar arrays for life-prediction purposes, this study is directed toward (a) developing a plan for predicting the service life of a specific solar array in a specific geographic site – viz., the 25-KW flat-plate array installed near Mead, Nebraska, and (b) developing technical information from laboratory and field measurements for designing an accelerated test that can be carried out in 2 years and have predictive validity for a service life as long as 20 years. More specifically, the objectives of the present study are to:

A. Develop Service-Life Prediction Plan

(1) Collect and analyze data on performance/time relationships encountered in the experience with present arrays in the field to provide engineering data for the test plan.

(2) Identify property/time/stress relationships most likely to relate array performance with time.

(3) Develop with the interacting agencies a field measurement plan to develop specific data with identified instrumentation on the Mead, Nebraska array.

(4) Using available engineering data and the previously developed methodology, develop for JPL approval a test plan for life prediction of the Mead, Nebraska array.

B. Implement Service-Life-Prediction Plan

(1) In conjunction with interacting agencies, acquire aging data according to the plan.

(2) Carry out selected laboratory experiments on modules or module materials to determine property/time aging relationships under overstressed conditions.

(3) Predict from the data analyses the expected service life of the array.

(4) Recommend on the basis of the analyses, plan procedures leading to a realistic accelerated test for mature designs of arrays.

STRESS SEVERITY RATINGS

As has been reported earlier in this study (see DOE/JPL-954328-78/10, "Development of Accelerated Test Design for Service Life Prediction of Solar Array at Mead, Nebraska, November 3, 1978) several environmental stresses will possibly be interactive in their contribution to long-term degradation of solar modules. These include: ultraviolet radiation; humidity; atmospheric contaminants of which SO_2 has been adopted as an example; mechanical forces arising from external sources (such as wind); temperature; and cyclic temperature. For the early steps in accelerated test design, these stresses have been dealt with in two groups. One group involves constant temperature; the other group involves cyclic temperature. The other four stresses are common to both groups.* Taking one of these sets of five stresses and assigning to each stress two levels, one high and one low for purposes of accelerated test design, $2^5=32$ separate experiments would be required to carry out a complete factorial test involving all combinations of these stresses at two levels each. As has been discussed in Study 4 of this contract (ERDA/JPL-954328-77/1, "Methodology for Designing Accelerated Aging Tests for Predicting Life of Photovoltaic Arrays, February 1, 1977) to conserve time and effort it is vital, where possible without impairing unduly the quality of the resulting information, to eliminate those tests which will not yield essential information. One step in the process of rationally reducing the number of tests required is to establish on the basis of sound technical judgment a relative rating of the severity of each of the 32 possible combinations of stresses as contributors to module degradation.

Table 1 lists the judgmental stress severity ratings for the 32 possible combinations of a set of five stresses for increase in cell series resistance at constant temperature, just one of several potentially important degradation modes for solar modules. The five stresses are temperature, ultraviolet radiation, SO_2, relative humidity and mechanical force. These stress severity ratings may be subjected to a Yates analysis, as discussed in the previously cited Study 4 report, as a means of identifying more clearly which of the stresses and stress combinations are judged to be of importance and which may possibly be eliminated from consideration in the test design. The second column in Table 1 contains results of a Yates analysis, and quantifies the relative importance of the main effects and interactions listed in the last column of Table 1.

While the stress severity ratings are key factors in the design of accelerated aging tests, it is clear from a perusal of Table 1 that neither they nor the quantification of main effects and interactions are subject to easy interpretation in connection with test design. However, interpretation can be aided by using a hierarchical tree representation of the main effects and interactions to assess the severity of stresses and the probable importance of these stresses in relation to the degradation mode or modes in question. The hierarchical tree representation of the data presented in Table 1 will be found in Figure A-2 of Appendix A**. The hierarchical tree is generated by first noting that the most important main effect is shown to be temperature. This is shown in column 2 of Table 1 by the entry 37.0 that corresponds to temperature; the other main effects are seen to be 10.5 for mechanical, 31.4 for relative humidity, 14.2 for SO_2, and 4.0 for UV. Because temperature is the most important main

*Stresses such as thermal shock, cell back bias, hail, abrasion, and accumulated surface dirt are not being left out of consideration. Actually they are very important. However, at this point they are judged to be largely non-interactive stresses and therefore amenable to different treatment.

**Some brief comments on the interpretation of hierarchical trees will be found at the beginning of the Appendix.

TABLE 1. STRESS SEVERITY AND MAIN EFFECTS AND INTERACTIONS FOR INCREASE IN CELL SERIES RESISTANCE – CONSTANT TEMPERATURE

Stress Severity Ratings*	Sum of Squares	Main Effects and Interactions
1.5	42.7	Mean
9.0	10.5	M**
23.9	31.4	RH
34.3	0.8	RH x M
9.0	14.2	SO_2
19.4	0.7	SO_2 x M
35.8	3.3	SO_2 x RH
46.3	-0.1	SO_2 x RH x M
3.0	4.0	UV
11.9	0.1	UV x M
28.4	0.7	UV x RH
38.8	0.1	UV x RH x M
11.9	0.4	UV x SO_2
22.4	0.3	UV x SO_2 x M
40.3	0.1	UV x SO_2 x RH
52.2	0.3	UV x SO_2 x RH x M
29.9	37.0	T**
40.3	0.4	T x M
60.0	4.9	T x RH
72.0	0.1	T x RH x M
41.8	3.3	T x SO_2
52.2	-0.1	T x SO_2 x M
82.1	1.9	T x SO_2 x RH
94.0	0.3	T x SO_2 x RH x M
34.3	0.3	T x UV
43.3	0.3	T x UV x M
65.0	-0.4	T x UV x RH
75.0	0.1	T x UV x RH x M
46.3	0.1	T x UV x SO_2
56.7	0.3	T x UV x SO_2 x M
86.6	0.1	T x UV x SO_2 x RH
100.0	0	T x UV x SO_2 x RH x M

*Normalized to 100.

**M and MCH are used interchangeably in this report to denote mechanical force. Likewise T and TMP both denote temperature.

effect, the hierarchical tree shows temperature as the splitting variable at the top of the tree. To determine the next most important variables the severity ratings are next split into two groups, one group corresponding to high temperature and one group corresponding to low temperature. A new Yates analysis is then performed for each of these groups to determine the variable that has the largest main effect. In the present case it is found that relative humidity has the largest main effect for both groups. This means that relative humidity is found to be the second most important variable, regardless of whether temperature is at a high level or at a low level. The hierarchical tree then shows relative humidity as the second splitting variable for both branches of the temperature split. This process is then continued to obtain the remainder of the hierarchical tree. That is, after each split a Yates analysis is made to determine the largest main effect, and the process continues until each branch of the tree terminates in one of the 32 stress combinations. Further details on these trees and their derivation are also discussed in the previously cited Study 4.

Most of the discussion of the relative severity of stresses and combinations of stresses in the remainder of this report will be centered around hierarchical trees. The hierarchical tree representation is a useful *tool* for dealing with the stress severity ratings.

Individual Degradation Modes

Table 2 lists those degradation modes for the Mead-array modules (Block II modules from two manufacturers) which at this point are judged to be most important.

TABLE 2. IMPORTANT DEGRADATION MODES IN THE TWO TYPES OF BLOCK II MODULES IN THE MEAD ARRAY

Surface accumulation of dirt
*Decrease in transmission
*Series resistance increase
*Delamination
*Cell cracking
*Interconnect corrosion
*Interconnect breakage
Electrical breakdown

The asterisked items in Table 2 are those degradation modes which have been selected for consideration in conjunction with the groups of possibly interactive stresses identified earlier (top of page 4).

As discussed in the last quarterly report (DOE/JPL-954328-78/10), several scientists on the BCL staff independently generated severity ratings for sets of stresses relative to the degradation modes asterisked in Table 2. Subsequently, the judgments of these scientists were combined to evolve a "composite" set of stress severity ratings for each degradation mode considered. The hierarchical trees representing the main effects and interactions for the individual degradation modes appear in Appendix A as Figures A-1 through A-11.

The development of stress severity ratings for a given degradation mode in a solar module requires a careful consideration of the stresses and their magnitudes to which the module is to be exposed, and of the possible contribution which those stresses might make to the mode of degradation in question. In the course of this consideration, the relative importance of individual stresses with respect to the degradation mode in question are often clarified and important combinations of stresses or interactions between stresses are identified. The following sections summarize the reasoning associated with the development of the stress severity ratings for each degradation mode considered.

Decrease in Transmission – Constant Temperature

Relative to this degradation mode the five stresses have been characterized as follows:

UV (Ultraviolet Radiation)	– driving
T (Temperature)	– important
RH (Relative Humidity)	– important
SO_2 (Concentration)	– small effect
M (Mechanical)	– very small effect

The following considerations have influenced this characterization:

(1) The effects considered include bulk effects in the silicone, adhesives, and AR coatings of the two types of modules in the Mead array.

(2) Increase in scattering as well as increase in absorption, α, are probably significant.

(3) Effects of surface accumulation of dirt are not included.

(4) UV appears to discolor (yellow) silicones. (Creates defects, vacancies.)

(5) High T may help to anneal UV-introduced defects although it is doubtful that T is high enough to have much effect in this regard.

(6) RH and T may contribute to bleaching of SiO_x AR coatings and, to a possibly lesser degree, bleaching of Ta_2O_5 AR coatings.

Cyclic temperature was considered not to change these effects in an important way.

Increase in Cell Series Resistance – Constant Temperature

Relative to this degradation mode the five stresses have been characterized as follows:

T	– important
RH	– important
SO_2	– important
M	– possibly significant
UV	– small effect if any

The following considerations have influenced this characterization:

(1) T x RH (the interaction between temperature and relative humidity) is considered to be the driving stress through corrosion.

(2) SO_2 or similar contaminants are important but generally require the presence of moisture to impart their most serious damage.

(3) The effect of T $>$ the effect of RH. The RH at Mead is never extremely low; therefore, corrosive potentialities are almost always present for stimulation by high T.

(4) Degradation of the metallization – Si bond or other metallization interfaces, i.e., Ni/Pb-Sn, are potentially very important. Possible causes include corrosion, mechanical stress, and differential thermal expansion.

<u>Increase in Cell Series Resistance –
Cyclic Temperature</u>

Relative to this degradation mode the five stresses have been characterized as follows:

T_c	–	important
RH	–	important
SO_2	–	significant
M	–	possibly significant
UV	–	small effect if any

The following considerations have influenced this characterization:

(1) T_c x RH is considered to be the driving stress through corrosion.

(2) SO_2 or similar contaminants are important, but generally require the presence of moisture to impart their most serious damage.

(3) If cyclic temperature enhances net transport of moisture into the module, degradation may be more severe than in the constant temperature case.

(4) Degradation of the metallization – Si bond or other metallization interfaces, i.e., Ni/Pb-Sn, are potentially very important. Possible causes include corrosion, mechanical stress, and differential thermal expansion.

<u>Delamination – Constant Temperature</u>

Relative to this degradation mode the five stresses have been characterized as follows:

T	–	driving
RH	–	driving
UV	–	driving
M	–	little effect
SO_2	–	some possible effect

The following considerations have influenced this characterization:

(1) T is expected to be a more degrading stress than RH.

(2) Interfacial forces arising from differential thermal expansion are expected to be important.

(3) Bond-degrading chemical and photochemical reactions are possible in the presence of moisture, SO_2, and UV.

Corrosion and delamination are occasionally observed to occur simultaneously at a given location. Corrosion could be the initial event leading to delamination as a result of chemical reaction. Alternatively delamination could be the initial event creating an interfacial void where corrosive contaminants can collect in contact with a metal surface. The first of these possibilities is considered the more likely.

<u>Delamination – Cyclic Temperature</u>

Relative to this degradation mode the five stresses have been characterized as follows:

T_C	–	driving
RH	–	important
UV	–	important
M	–	small effect
SO_2	–	some possible effect

The following considerations have influenced this characterization:

(1) T_C x RH is expected to be at least as severe a stress combination as T_C x UV and probably more so.

(2) Apart from possible corrosive effects T_C x RH may produce internal freeze – thaw phenomena contributing to delamination.

(3) Interfacial forces arising from differential thermal expansion are expected to be important.

(4) Bond-degrading chemical and photochemical reactions are possible in the presence of moisture, SO_2, and UV.

Corrosion and delamination are occasionally observed to occur simultaneously at a given location. Corrosion could be the initial event leading to delamination as a result of chemical reaction. Alternatively delamination could be the initial event creating an interfacial void where corrosive contaminants can collect in contact with a metal surface. The first of these possibilities is considered the more likely.

If cyclic temperature enhances net transport of moisture into the module, degradation occurring as a result of some of the above phenomenon may be more severe than in the constant-temperature case.

Cell Cracking – Constant Temperature

Relative to this degradation mode the five stresses have been characterized as follows:

T	–	driver
M	–	driver
RH	–	little or no effect
SO_2	–	little or no effect
UV	–	little or no effect

The following considerations have influenced this characterization:

(1) T is expected to be a more important contributor to cell cracking than M alone or than M in combination with the other stresses.

(2) Frame ribs and similar structural features can probably contribute to cell cracking.

(3) Impact damage from hail probably contributes some to cell cracking. However, impact damage is not included among the stresses considered here.

Cell Cracking – Cyclic Temperature

Relative to this degradation mode the five stresses have been characterized as follows:

T_c	–	driver
RH	–	potentially very important
M	–	important
SO_2	–	no effect
UV	–	no effect

The following considerations have influenced this characterization:

(1) T_c is expected to be a more degrading stress than the combination RH x M as a result of differential thermal expansion.

(2) Frame or substrate ribs and similar structural features are expected to contribute to cell cracking under cyclic temperatures.

(3) Freezing of moisture internal to the module or freeze – thaw phenomena are potential hazards under cyclic temperatures. Thus, T_c x RH is expected to be a more severe stress combination than T_c x M.

Internal freezing could, however, make T_c x M a troublesome stress combination.

An important and as yet unanswered question in connection with this degradation mode centers around the relative severity of high-temperature and low-temperature stresses.

Interconnect Corrosion – Constant Temperature

Relative to this degradation mode the five stresses have been characterized as follows:

RH – driving
SO_2 – driving
T – driving
UV – possible effect
M – no effect

The following considerations have influenced this characterization:

(1) In stress severity RH is expected to be $\geqslant SO_2$.

(2) The simultaneous presence of high levels of moisture, SO_2, and T should be quite severe.

(3) Photochemical reactions may occur under UV radiation in the presence of moisture and SO_2 at interconnect surfaces.

Interconnect corrosion may be accompanied by delamination at the same location. It is judged more probable that corrosion leads to delamination than the reverse.

Interconnect Corrosion – Cyclic Temperature

Relative to this degradation mode the five stresses have been characterized as follows:

RH – driver
T_c – driver
SO_2 – driver
UV – little effect
M – no effect

The following considerations have influenced this characterization:

(1) In stress severity RH x T_c x SO_2 should exceed RH x T_c.

(2) If cyclic temperature enhances net transport of moisture into the module, degradation may be more severe than in the constant temperature case.

(3) Photochemical reactions may occur under UV radiation in the presence of moisture and SO_2 at interconnect surfaces.

Interconnect corrosion may be accompanied by delamination at the same location. It is judged more probable that corrosion leads to delamination than the reverse.

Interconnect Breakage – Constant Temperature

Relative to this degradation mode the five stresses have been characterized as follows:

T	–	driver
M	–	driver
RH	–	possibly some effect
SO_2	–	possibly some effect
UV	–	little effect

The following considerations have influenced this characterization:

(1) T x M is expected to be a more severe stress than RH x SO_2 x UV.

(2) T is expected to be a more severe stress than M x RH x SO_2 x UV through differential thermal expansion.

Corrosion may precede interconnect breakage in some instances.

Interconnect Breakage – Cyclic Temperature

Relative to this degradation mode the five stresses have been characterized as follows:

T_c	–	driver
RH	–	driver
M	–	potentially important
SO_2	–	little or no effect
UV	–	little or no effect

The following considerations have influenced this characterization:

(1) T_c x RH is expected to be a more severe stress than T_c x M.

(2) Differential thermal expansion and freezing of moisture at critical locations internal to the module are possible hazards.

If cyclic temperature enhances net transport of moisture into the module degradation may be more severe than in the constant temperature case.

Corrosion and/or delamination may precede interconnect breakage in some instances.

Combining Degradation Modes

Once the probable degradation modes are identified along with the stresses and stress magnitudes that affect the modes in a sensitive way, three important steps immediately follow in the accelerated test design. The first is to identify any stresses from among those to be used which would be very difficult or costly to apply in conjunction with other stresses in a large-scale experiment. There are particular problems of this type with two stresses under

consideration here. It would be both costly and technically difficult to expose an array of test modules to ultraviolet radiation at the intensities contemplated for accelerated test purposes while simultaneously exposing the modules to temperature, humidity, and chemical contaminants. While ultraviolet radiation certainly has potential for interacting with other stresses, it is recommended that ultraviolet radiation as a stress be separated from the main body of the planned test procedure and handled separately with special precautions to insure satisfactory consideration for it.

Likewise mechanical force applied to large numbers of modules simultaneously with high temperature, relative humidity, and chemical contamination presents formidable problems. It is therefore recommended that it too be separated from the main body of the planned test for special handling.

Thus far in the development of the accelerated test plan the relative severities of the stresses under consideration have been evaluated largely in relation to individual degradation modes. As the second step, it is necessary to amalgamate that information into a single picture of module degradation from all modes simultaneously when subjected to various combinations of stress intensities.

As the third step, it is necessary to eliminate from consideration tests associated with those combinations of stresses which analysis and judgment suggest will be insignificant relative to other combinations in their effect on module performance.

It has been declared desirable for technical as well as economic reasons to plan the final test design to provide for exposure of modules to ultraviolet radiation separate from other stresses insofar as is possible. Reviewing the hierarchical trees in Figures A-1 through A-11 (Appendix A), it can be seen that ultraviolet is very important in its anticipated effect on decrease in transmission (see Figure A-1), but does not occur higher than the third level in any of the other trees.* Therefore the tree in Figure A-1 will provide a basis for part of the final test design. On the basis of that tree, it appears that mechanical stress and SO_2 stress can be expected to have very little effect. It is therefore concluded that they can be safely pruned from the tree. It is also concluded that the relative-humidity stress in the high-ultraviolet, high-temperature branch of the tree must at this stage be retained. The relative-humidity stresses in the other three branches of the tree may tentatively be pruned. Results of early experiments must be monitored closely to determine if reversal of this conclusion is dictated.

With these conclusions, the pruned tree shown in Figure 1 is presented as offering the simplest possible array of experiments dealing with the anticipated degrading effects of ultraviolet radiation. It obviously could not be dealt with to the complete exclusion of temperature as a condition of the test. Furthermore it appears unwise to completely exclude relative humidity as an accompanying stress without experimental justification for doing so. These requirements suggest the execution of some initial experiments on minimodules or other special samples in this portion of the test plan.

Mechanical force is the other stress identified for separate treatment because of technical and economical problems. Reviewing Figures A-2 through A-11, it is observed that mechanical force occurs higher than the third level only in Figures A-6 and A-10 where it occurs at the second level following temperature in both cases. The tree in Figure A-6 reflects a quite low

*See later discussion on delamination.

Specified Degradation Mode:

Decrease in Transmission – Constant Temperature.

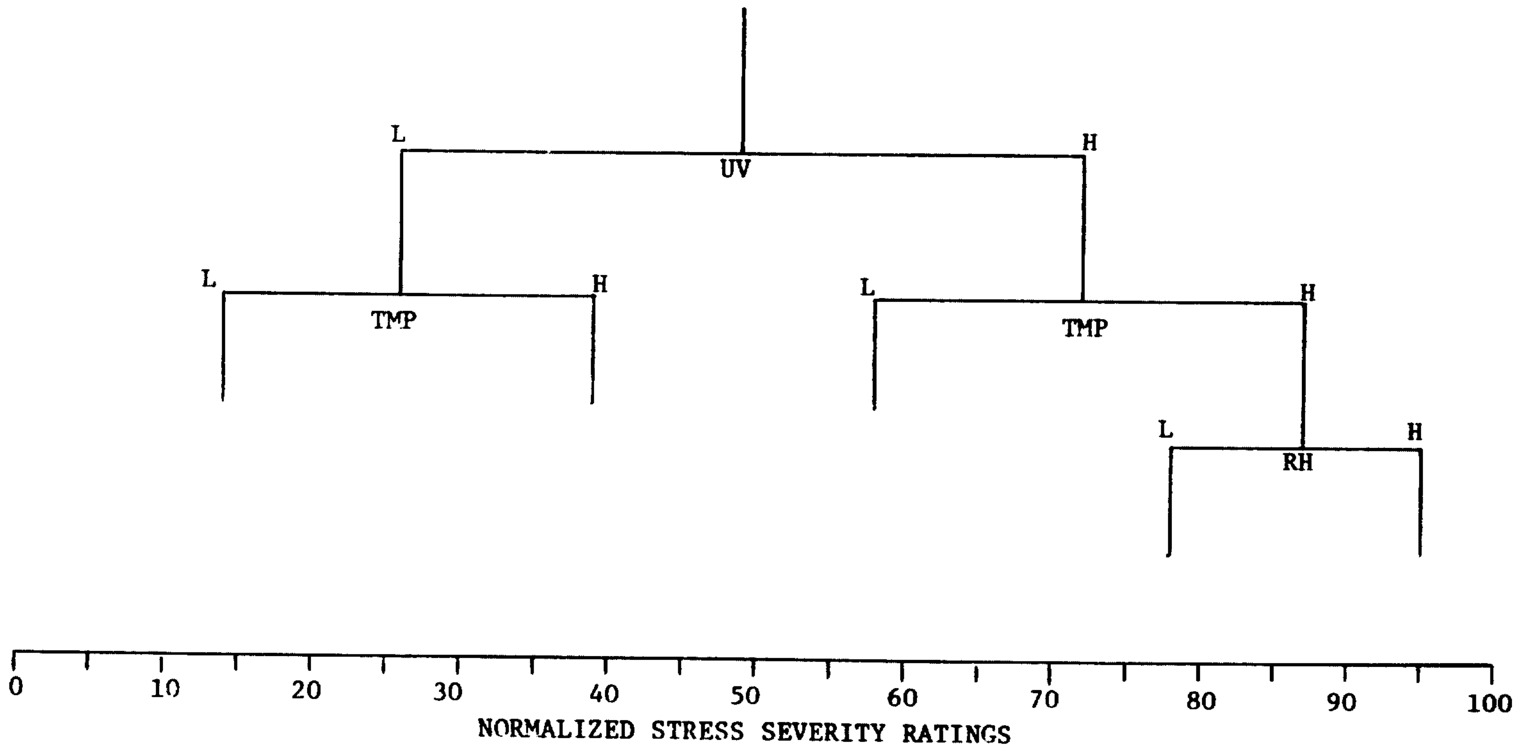

FIGURE 1. THE HIERARCHICAL TREE ASSOCIATED WITH THE SPECIFIED DEGRADATION MODE

sensitivity to ultraviolet radiation as well as to stresses further down the tree. The tree can therefore tentatively be pruned of everything beyond the mechanical stresses. Likewise the tree in Figure A-10 reflects relatively small sensitivity to relative humidity as well as all stresses further down the tree. Hence pruning all stresses beyond mechanical force may be justified here. Assuming that is the case the remaining portions of these two trees can be combined to form the tree shown in Figure 2. That tree is proposed to represent the portion of the test plan dealing with the major effects of mechanical force. The effects are expected to occur primarily in cell cracking at constant temperature and in interconnect breakage at constant temperature. It is believed that early experiments should evaluate the possible effect of relative humidity at high temperature and high mechanical stress on interconnect breakage to confirm that the tree has not been too severely pruned.

The remaining eight trees, those in Figures A-2, A-3, A-4, A-5, A-7, A-8, A-9, and A-11, exhibit some useful similarities. In Figures A-2, A-3, A-4, A-5, A-6, and A-11, the first split occurs on temperature and the second on relative humidity at both the low and high temperatures. In Figure A-9 the first split occurs on relative humidity and the second on temperature. In Figure A-8 the first split occurs on relative humidity, the second on SO_2 and the third on temperature. Advantage can be taken of these similarities to devise a composite tree involving three variables, temperature, relative humidity, and SO_2 pruned as shown in Figure 3 and representing the eight degradation modes identified in that figure.

One note of caution must be cited in connection with this tree. For cell cracking under cyclic temperatures (Figure A-7) and interconnect breakage under cyclic temperature (Figure A-11), one should try to determine on the basis of early experiments the validity of pruning mechanical force in the presence of temperature and relative humidity from this portion of the test plan. If a sensitivity to mechanical force should be observed in these early tests, then the accommodation in the final test plan of cell cracking under cyclic temperatures and interconnect breakage under cyclic temperatures should be reconsidered.

With these judgments, one can contemplate a grouping of tests for the overall test design somewhat as shown in Table 3. Several remarks need to be made about this grouping. First of all, these groupings are tentative. As noted in *Future Work*, presented subsequently, the actual groupings and especially the number of stress levels employed will depend in part upon statistical considerations, that is, upon a selection of tests which give an acceptable minimum of confounding in estimating the parameters involved in the relationship between degradation rate and stress magnitudes.

The first two groupings represent a separation of the effects of constant temperature and temperature cycling. Groupings III and IV are inserted to test separately the major effects of ultraviolet radiation and mechanical forces.

In Groups I and II, note that cell forward bias is included as a surrogate for illumination. Accelerating the illumination between 0.4 and 1.1 μm is very difficult to accomplish experimentally and judged to be only of, at most, modest severity in aging the module. On the other hand, some degradation mechanisms – such as electrolytic corrosion – could be affected by current flow. Cell forward bias sufficient to generate 1-sun equivalent power output will furnish the current, although it is to be noted that the current will be in the opposite direction to that which obtains under sun illumination.

Specified Degradation Modes:

Cell Cracking - Constant Temperature

Interconnect Breakage - Constant Temperature*

---

* Possible effects of RH at high temperature and high mechanical stress should be checked.

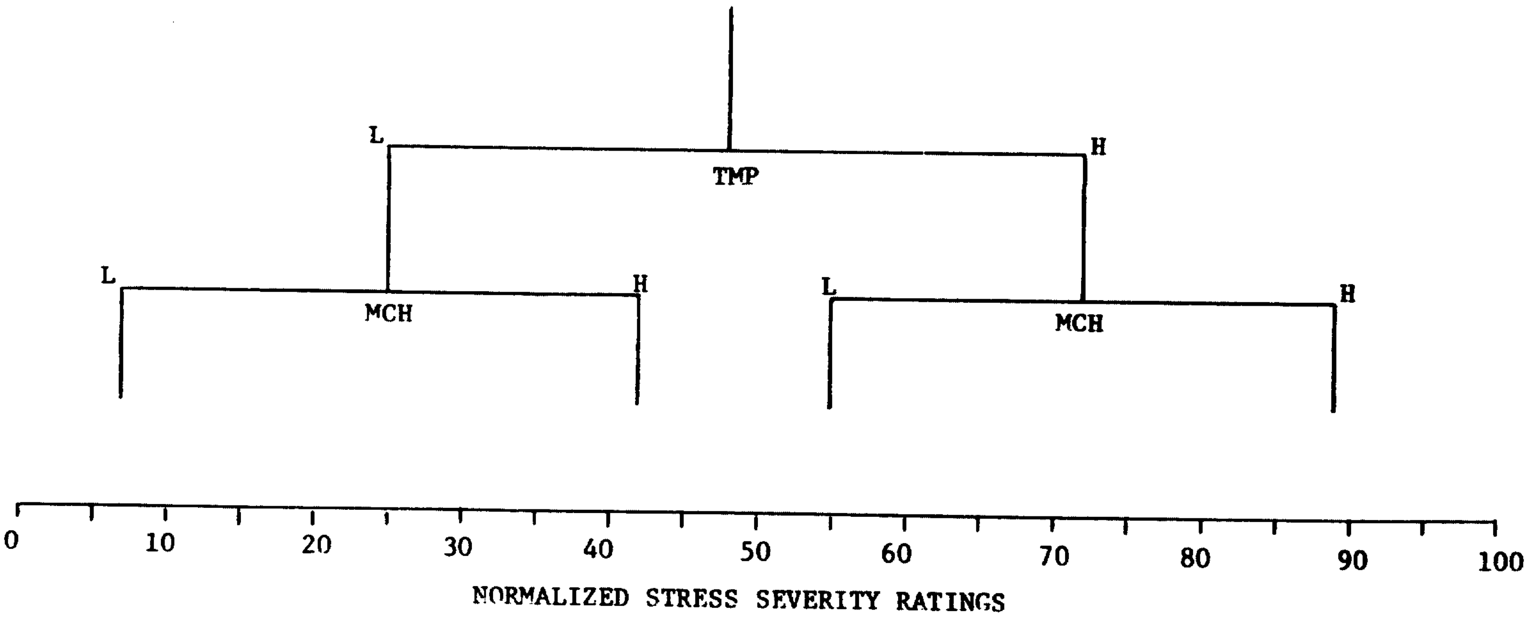

FIGURE 2. THE COMPOSITE HIERARCHICAL TREE REPRESENTING A SYNTHESIS OF TREES ASSOCIATED WITH THE TWO SPECIFIED DEGRADATION MODES

Specified Degradation Modes:

Increase in Series Resistance - Constant Temperature.

Increase in Series Resistance - Cyclic Temperature.

Delamination - Constant Temperature (excluding possible effects of UV).

Delamination - Cyclic Temperature (excluding possible effects of UV).

Cell Cracking - Cyclic Temperature (excluding possible effects of mechanical stress*).

Interconnect Corrosion - Constant Temperature.

Interconnect Corrosion - Cyclic Temperature.

Interconnect Breakage - Cyclic Temperature (excluding possible effects of mechanical stress*).

---

* Make separate check on effects of mechanical stress in presence of temperature and humidity stresses. If no special effects occur then this type of test array should accommodate this degradation mode. If special effects do occur then the accommodation of this degradation mode should be reconsidered.

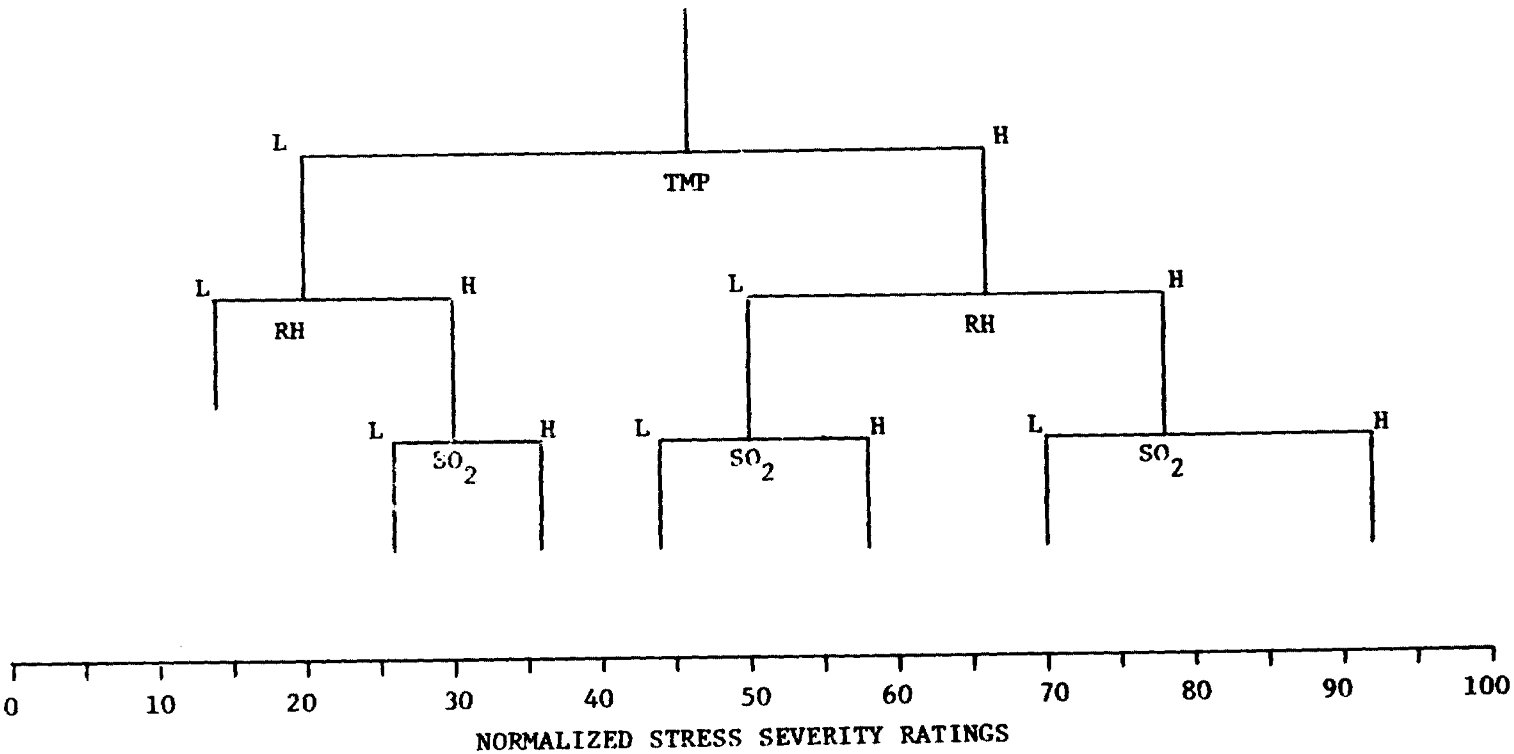

FIGURE 3. THE COMPOSITE HIERARCHICAL TREE REPRESENTING A SYNTHESIS OF TREES ASSOCIATED WITH THE EIGHT SPECIFIED DEGRADATION MODES

TABLE 3. PROPOSED GROUPING OF TESTS

Stresses	Magnitudes
I. Constant Temperature	30, 72, 86, 95 (C)
Relative Humidity	60, 95 (%)
SO_2 Concentration	5, 50 (ppb)
Forward Bias	1-sun equivalent power
Cell-to-Frame Bias	1500 (V)
II. Temperature Cycling	25 (±30), 45 (±50), -8 (±32) (C)
Relative Humidity	at Mean T: 60, 95, 60 (%)
SO_2 Concentration	5, 50 (ppb)
Forward Bias	1-sun equivalent power
Cell-to-Frame Bias	1500 (V)
III. Ultraviolet Radiation	5, 50 (suns)
Temperature	40, 85 (C)
Relative Humidity	95 (%)
IV. Mechanical Force	(Judgments yet to be made)
Temperature	
Relative Humidity	

Also in Groups I and II, a fixed dc voltage of 1500 volts between cells and frame is to be noted. Since the Mead Array operates at approximately 200 volts, such a fixed bias is judged sufficient to expose voltage-breakdown events, as well as surface discharges brought on primarily by condensed water and "dirt".

The grouping involving temperature cycling, Group II, calls for cycling around several "mean" temperatures, 25, 45, and -8 C. All combinations of Group-II tests would not be evaluated. The aim is to test those conditions contributing primarily to delamination and the effects of the freeze-thaw cycles. The relative humidity would be set at the mean temperature and would subsequently vary at the temperature varied. For example, if the relative humidity is set at 60 percent at the mean temperature of 25 C, it would decrease to 12 percent at the upper temperature extreme (55 C) and increase to 100 percent at approximately 17 C and remain at this value down to the lower temperature extreme of -5 C. These values are based on the saturated partial pressure of water vapor over liquid water. All conditions in Group II would encompass the freeze-thaw cycle.

As stated previously, accelerated aging by ultraviolet radiation presents particular problems experimentally. Group III tests will undoubtedly require separate experimental test specimens. The problem will be to choose a specimen size small enough such that the specimen can be

illuminated with available and appropriate sources (0.3 to 0.4 μm) but large enough to simulate the effects on a full-sized module. At present, it is felt that single encapsulated cells will be appropriate specimens, but this point will have to be assessed continuously through the group tests.

No conclusions have been made as yet with regard to the mechanical tests (Group IV), other than that the static and cyclic nature of mechanical forces must be considered and that temperature can play an important role in determining the extent of degradation by such forces. Relative humidity might also be important but perhaps to a lesser extent.

Functional Relationships Between Degradation Modes and Stress Magnitudes

Up until now the primary efforts in the test-design development have centered on only two levels of stress magnitudes (see Table 6 of DOE/JPL-954328-78/10) to assess the severity ratings for each degradation mode and for combined modes. At least for some stresses (temperature, for example), more than two levels of stress magnitudes will be required to give statistical validity to the test design and life prediction. To be able to space the levels in magnitude over a range within which the degradation mode at overstress is the same under normal stress, it is highly desirable to make judgments about the form of functional relationships between degradation modes and stress magnitudes. Moreover, the more one knows about the form of these relationships, the better one is able to choose appropriate functional forms to trial-fit the eventual test data. Some tentative suggestions are made about the form of the functional relationships for the information in Figures 1, 2, and 3.[a]

(1) Decrease in transmission

$$= f[I_{uv}^{m},(RH)T\ \exp(-E_1/kT)]$$

where:

I_{uv} = ultraviolet intensity

m = an as yet unassigned power

RH = relative humidity

T = temperature

E_1 = an activation energy for the operative reaction

k = the Boltzmann constant

(a) In the succeeding section of this report, a more general formulation of the functional relationships is given as a model. There the rate of degradation, R, is related to a functional form of the type:

$$R = C(\exp{-B/T})s_1^{n_1}s_1^{n_2}\ldots s_m^{n_m}, \text{ where}$$

C, B, and n's are constants, the s's are stress magnitudes, and T is the temperature.

(2) Occurrence of cell cracking under constant temperature stress

$$= f(T, M)$$

where

M = mechanical force above some yet to be determined threshold.

(3) Occurrence of interconnect breakage under constant temperature stress

$$= f(T, M)$$

(4) Increase in cell series resistance under constant-temperature stress

$$= f\left\{[SO_2](RH)T \exp(-E_2/kT)\right\}$$

where

$[SO_2]$ = atmospheric concentration of SO_2
E_2 = an activation energy for the operative reaction

(5) Occurrence of delamination under constant temperature stress

$$= f\left\{T, [SO_2](RH)T \exp(-E_3/kT)\right\}$$

where

E_3 = an activation energy for the operative reaction

(6) Extent of interconnect corrosion under constant temperature stress

$$= f\left\{[SO_2](RH)T \exp(-E_4/kT)\right\}$$

where

E_4 = an activation energy for the operative reaction

(7) Increase in cell series resistance under cyclic temperature

$$= f\left\{[SO_2](RH)\bar{T} \exp(-E_2/k\bar{T}_c)\right\}$$

where

$\bar{T}_c$ = the mean value of the cyclic temperature range

(8) Occurrence of delamination under cyclic-temperature stress

$$= f\left\{\Delta T_c, n_c(RH), [SO_2](RH)\bar{T}_c \exp(-E_3/k\bar{T}_c)\right\}$$

where

ΔT_c = the magnitude of the cyclic temperature range
n_c = the number of temperature cycles

(9) Occurrence of cell cracking under cyclic temperature stress

$$= f[\Delta T_C, n_C(RH)]$$

(10) Extent of interconnect corrosion under cyclic-temperature stress

$$= f \left\{[SO_2](RH)\bar{T}_c \exp(-E_4/k\bar{T}_c)\right\}$$

(11) Occurrence of interconnect breakage under cyclic temperature stress

$$= f[\Delta T_C, n_C(RH)]$$

Note that the same activation energy is assumed for increase in cell series resistance under constant and cyclic temperature stresses. Similar assumptions have been made for delamination and interconnect corrosion under the two types of temperature stresses.

DEVELOPMENT OF A MODEL FOR THE DESIGN AND ANALYSIS OF MULTISTRESS ACCELERATED AGING TESTS

In the previous Study 4 report(1) a methodology is presented for identifying a set of overstress aging tests suitable for predicting the service life of photovoltaic arrays. The methodology aims to reduce the number of tests ordinarily required by a complete factorial design, as noted previously in this report. The reduction is accomplished by using engineering knowledge to make explicit quantitative judgments concerning the relative importance of each possible test in terms of the anticipated severity of each test. The severity ratings for the possible tests are graphically represented in the form of a hierarchical tree. The form of tree then permits an explicit identification of which main effects and interactions it is most essential to determine by means of accelerated aging tests. Those test combinations of stress levels that are judged to be less essential are pruned from the tree and are consequently dropped from the experimental design. The resulting statistical design is degraded but can be analyzed using a mathematical model based on **conditional** main effects and interactions. Additional expositions of the methodology were presented at the DOE/NBS Workshop on the Stability of Thin Film Solar Cells and Materials(2), and at the Thirteenth IEEE Photovoltaic Specialists Conference – 1978(3).

Further innovative developments of the accelerated test methodology are summarized in the following paragraphs. The new developments combine a general multistress relation for degradation rates (Eyring model) with an assumed mathematical form for the degradation over time of the power output from a solar module. These results are subsequently shown to be related to the hierarchical tree.

The overall result of this new effort is a promising mathematical model and an associated graphical tree representation. It is believed that these tools can serve both as a basis for generating predicted or hypothesized experimental outcomes, when used in the experimental design stage, and for analyzing multistress accelerated test data, after the aging tests are performed.

Preliminary Assumptions

It is assumed that the aging of a solar module may be attributed to irreversible changes that result in a decrease in power output. The age of a module at any time can be expressed in terms of the percentage reduction at that time from the initial power output of the module. The age of a module is assumed to be highly nonlinear as suggested by the following sketch:

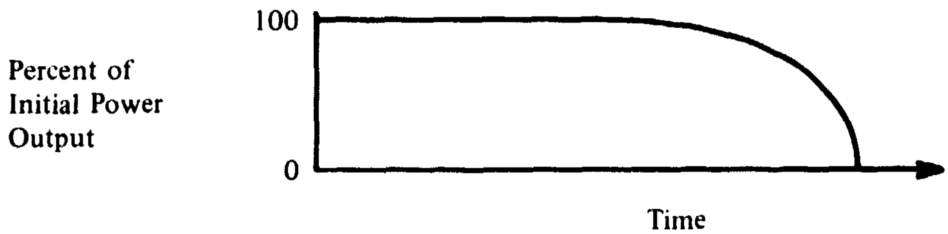

As indicated by the sketch, it is assumed that there is a small rate of loss of power output for a very long time period, but once a loss of power begins to occur, further losses will occur more

rapidly and will ultimately result in failure. It seems reasonable to suppose that any solar module that has a long expected service life will show a power output curve of this assumed form.

Degradation of Power Output

At constant temperature the degradation of power output is assumed to be representable in mathematical terms as follows:

$$P(t) = P_o[1-(S/S_o)^N(t/t_o)]^{1/N} \quad , \tag{1}$$

where

P(t) denotes the power output at time t,

P_o denotes the initial power output,

S denotes a constant applied nonthermal environmental stress,

t_o denotes the time required to obtain a significant power loss (failure) under a large overstress condition S_o, and

N denotes an overall endurance exponent.

In addition to representing the curve sketched above, this mathematical form can also be used to describe linear degradations over time, and degradations that are initially large but subsequently decrease more slowly over time. This mathematical form has been used by Simoni to describe voltage breakdown results obtained from accelerated life tests for a variety of insulation materials used for high-voltage cables.[4]

In order for Equation (1) to be useful, it is clear that it is necessary to construct a suitable measure of the constant overall nonthermal stress S. This means, for example, that it is necessary to have a single measure S that can represent the combined effect of a selected combination of low and high levels of RH, SO_2, and UV. A possible method for constructing such a measure is treated in a later paragraph.

Degradation Rate as a Function of Imposed Thermal and Nonthermal Stresses

The following mathematical model is assumed to describe the time rate of degradation of power output as a function of imposed stresses:

$$R = A\exp(-B/T)\exp[(k_{11}+(k_{12}/T))g_1(s_1) + \ldots + (k_{m1}+(k_{m2}/T))g_m(s_m)] \quad , \tag{2}$$

where

R denotes the time rate of degradation of power output,

T denotes absolute temperature,

$s_1, \ldots, s_m$ denote m imposed nonthermal stresses,

$k_{11}, k_{12}; \ldots; k_{m1}, k_{m2}$ denote m pairs of constants associated with the m nonthermal stresses,

A, B denote constants associated with the thermal stress (temperature), and

$g_1, \ldots, g_m$ denote m unknown functions corresponding, respectively, to the m nonthermal stresses (environmental stresses other than temperature).

In the literature associated with accelerated testing, Equation (2) is usually called Eyring's relation[5,6,7]. However, to the authors' knowledge, the relation has neither been rigorously proved nor formally published by Eyring. Instead, during the course of an early Battelle program involving accelerated testing, the relation was informally suggested by Eyring as a relation having a mathematical form that is consistent with general principles associated with the physics of rate processes.

It is next assumed that the unknown functions involved in Equation (2) can be expressed as follows:

$$g_j(s_j) = \ln s_j \ , \ j=1, \ldots, m \quad ,$$

where the s_j are dimensionless. This means that the quantitative effect of each nonthermal stress is assumed to be properly measured in terms of the natural logarithm of its dimensionless measure. Some limited support for such an assumption has been noted by Simoni[4], who shows that the empirically discovered capacitor law, $(\text{Voltage})^n \text{x} (\text{Life})$ = constant, can be deduced from the Eyring relation by using a logarithmic measure for the voltage stress.

The substitution of $\ln s_j$ for $g_j(s_j)$ in Equation (2) yields the following form for the time rate of degradation:

$$R = A \exp(-B/T) s_1^{\ n_1} \ldots s_m^{\ n_m} \quad , \tag{3}$$

where the temperature-dependent exponents are given by

$$n_j = k_{j1} + (k_{j2}/T), j=1, \ldots, m \quad .$$

In this form the degradation rate is seen to be expressed as proportional to a product of factors. The first factor, A exp(-B/T), corresponds to the Arrhenius relation and shows approximately how the degradation rate increases with temperature. The remaining factors correspond to the nonthermal stresses. The relation shows that the degradation rate R is proportional to a measure of each nonthermal stress raised to an appropriate power. It should be noted that these exponents are real numbers (not necessarily integers) and can be negative, zero, or positive.

Several comments concerning the simple form of Equation (3) should be made. It is not proposed that such a mathematical form for the degradation rate is rigorously correct. The form is too simple. In terms of a Taylor series expansion about a point, corresponding to a set of stress levels, $s_1, \ldots, s_m$, such a relation may prove to be adequate is some expansion region about the point, provided the region is not "too large". It may also be noted that the fitting of Equation (3) to accelerated test data at constant temperature would only require the estimation

of the exponents $n_1, \ldots, n_m$. However, when the temperature is varied, then, in addition to A and B, two parameters, k_{j1} and k_{j2}, must be estimated for each nonthermal stress. In a practical sense, it is anticipated that Equation (3) can serve as a reasonable parsimonious approximation to the true, but unknown, relation for the degradation rate. The approximation is expected to prove useful in the design of adequate accelerated tests and may also provide an initial global method for analyzing data obtained from accelerated life tests.

Endurance Exponents and Overall Measures for Nonthermal Stresses

Equation (3) indicates that the nonthermal stresses $s_1, \ldots s_m$ jointly affect the degradation rate as a product of powers: $s_1{}^{n_1} \ldots s_m{}^{n_m}$. Such a product suggests the desirability of defining a measure of the overall stress, S, and an endurance exponent, N, in such a way that

$$S^N = s_1{}^{n_1} \ldots s_m{}^{n_m} \quad . \tag{4}$$

It is not difficult to show that Equation (4) is satisfied if S is defined as follows:

$$S = s_1 \ldots s_m \quad , \tag{5}$$

and N is defined by the equation:

$$N = \sum_{i=1}^{m} (n_i \ln s_i) / \sum_{i=1}^{m} (\ln s_i) \quad . \tag{6}$$

These results show that an overall measure of the nonthermal stress is given by the product of the individual stress measures, and the endurance exponent for the overall nonthermal stress is obtained as a weighted average of the individual endurance exponents, where the weights are equal to the logarithmic measures of the individual stresses. Finally, because the s_j are assumed to be dimensionless*, it follows that S is also dimensionless.

Relation Between Changes in Nonthermal Stress Levels and the Resulting Change in Degradation Rate

At a constant temperature let the degradation rate, r, be written as follows:

$$r = Ks_1{}^{n_1} \ldots s_n{}^{n_m} \quad , \tag{7}$$

where K is a parameter that absorbs the Arrhenius factor in Equation (3). Now suppose that the dimensionless measure of each stress is incremented, so that s_j is replaced by $(s_j + ds_j)$, where the increment ds_j is negative, zero, or positive. Let the resulting increment for the degradation rate be denoted by dr so that:

$$r+dr = K(s_1+ds_1) \ldots (s_m+ds_m) \quad .$$

*For s_j to be dimensionless, assume the s_j's are divided by some reference value. See later discussion.

This relation can be rewritten as follows:

$$r(1+(dr/r)) = K[s_1(1+(ds_1/s_1))]^{n_1} \quad ,$$

$$\ldots [s_m(1+(ds_m/s_m))]^{n_m} \quad ,$$

and division of this result by Equation (7) yields

$$[1+(dr/r)] = [1+(ds_1/s_1)]^{n_1} \ldots [1+(ds_m/s_m)]^{n_m} \tag{8}$$

Roughly, this equation shows how percentage changes in the "input" stress levels affect the percentage change in the "output" degradation rate. Clearly, if all ds_j/s_j are set equal to zero, then no change occurs in the degradation rate. Thus, in addition to a low and a high level for each stress, this relation suggests the desirability of having an intermediate "reference" level. When all stresses assume their reference values, the corresponding degradation rate is also taken to assume its reference value which is arbitrarily set equal to 1.0. Percentage changes from the reference values can then be interpreted unambiguously for both the individual stress levels and the associated degradation rate.

Equation (8) also indicates the important role of the endurance exponents. For a given percentage change in each nonthermal stress, that nonthermal stress having the largest endurance exponent will have the greatest affect on the degradation rate.

In order to relate Equation (8) to hierarchial trees, it is convenient to make another transformation. Let s_j' and s_j'' denote the low and high levels of the stress s_j, $j=1, \ldots m$. Also, let s_j^o denote an intermediate reference stress obtained by taking the geometric mean of s_j' and s_j'':

$$s_j^o = (s_j' s_j'')^{1/2}, j = 1, \ldots, m \quad .$$

Then for the low level of stress:

$$ds_j/s_j = (s_j' - s_j^o)/s_j^o = (s_j'/s_j^o)-1 \quad ,$$

so that

$$1+(ds_j/s_j) = s_j'/s_j^o$$

Similarly, for the high level of stress, it is found that

$$1+(ds_j/s_j) = s_j''/s_j^o \quad .$$

Thus, a factor $[1+(ds_j/s_j)]$ appearing in Equation (8), and representing a low or high stress level, may be replaced by the ratio s_j'/s_j^o, or by s_j''/s_j^o, respectively. Because $s_j^o = (s_j' s_j'')^{1/2}$, it is easily seen that

$$s_j''/s_j^o = (s_j'/s_j'')^{1/2}$$

and

$$s_j'/s_j^o = (s_j''/s_j')^{1/2} \quad .$$

Putting

$$f_j = (s_j'/s_j'')^{1/2} \quad ,$$

it follows that

$$f_j^{-1} = (s_j''/s_j')^{1/2} \quad ,$$

and consequently, every factor in Equation (8) is equal to $f_j^{n_j}$ if it represents the high level of the jth stress and is equal to $f_j^{-n_j}$ if it represents the low level of the jth stress. Both of these cases may be symbolized by $f_j^{\delta m_j}$ where δ equals -1 or 1 for low or high stress levels, respectively.

Summarizing, Equation (8) can now be written as follows:

$$1+(dr/s) = f_1^{\delta_1 n_1} \ldots f_m^{\delta_m n_m} \quad , \tag{9}$$

where

$$f_j^{\delta_j n_j} = \begin{cases} (s_j''/s_j')^{n_j/2}, \text{ for a high level of the jth stress} \\ (s_j'/s_j'')^{-n_j/2}, \text{ for a low level of the jth stress.} \end{cases}$$

A general split in a hierarchical tree can now be labeled as shown in the following sketch:

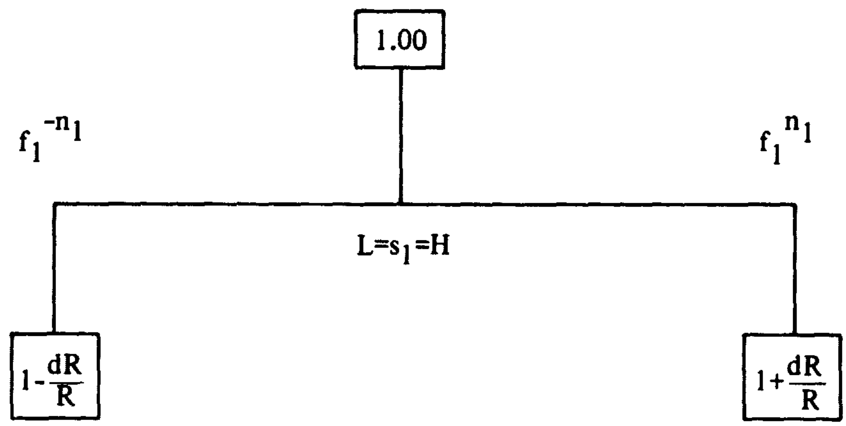

The sketch shows that the split is made on stress s_1, with the low and high levels of the stress associated with the left and right branches, respectively. The entries inside the boxes represent the values of the degradation rate relative to its reference value. At the top of the tree the entry 1.00 indicates that the degradation rate is at its reference level. The entry 1+(dR/R) in the right branch indicates that the degradation rate is increased by the increment dR/R when the stress s_1 takes its high level. Similarly, the degradation rate is decreased by dR/R when s_1 takes its low level. These percentage changes in the "output" degradation rates result from percentage changes in the "input" stress levels.

The numerical values for the percentage changes in the input stress levels are known because the high and low levels of each stress are defined prior to construction of the tree. The numerical values of the output percentages for the degradation rates may be obtained from the engineering estimates of the severity ratings under the assumption that percentage changes in severity ratings and degradation rates are numerically equal. That is, if engineering judgment indicates that a severity rating is increased by 10 percent when a particular stress is increased from its low level to its high level, then it is assumed that the degradation rate for power output is also increased by 10 percent.

Under these assumptions, percentage changes in the input stress levels and the resulting percentage changes in the output degradation rates can be numerically determined directly from the hierarchical tree. Moreover, estimates of the endurance parameters can also be obtained. As an example, suppose that a 5 percent increase in stress level, s_1, is associated with a 10 percent increase in degradation rate. It follows that

$$1 + (dR/R) = 1.10 = (1.05)^{n_1} = f_1^{\ n_1} \quad ,$$

and this relation may be solved for the endurance exponent to obtain

$$n_1 = \ln(1.10)/\ln(1.05) = 1.95 \quad ,$$

so that

$$1.10 = (1.05)^{1.95} \quad .$$

In a similar manner, the endurance exponents can be computed for each split in the hierarchical tree. In general, these endurance exponents serve to transform the percentage changes in input stress levels to corresponding percentage changes in the output degradation rates.

A Numerical Example

The following sketch shows a numerical example for the hierarchical tree. The sketch indicates that cyclic temperature is the first splitting variable and that relative humidity is the second splitting variable for each branch of the tree. At the first split the tree shows that, relative to its reference value of 1.0, the degradation rate of power output increases by 60 percent at the high level of the cyclic temperature stress. This increase in the degradation rate is seen to be the result of a 34 percent increase in the thermal stress level, which has an estimated n-value of 1.61 obtained by solving $1.60 = (1.34)^n$ for n. The next split along the right branch of the tree shows that a 54 percent increase in the level of relative humidity is associated with a 32 percent increase in the degradation rate for power output, with an n-value of 0.64. The left branch of the tree is interpreted in a similar manner.

The following relations may also be noted:

(1) The product of the two [1 + (dR/R)] factors at each split is equal to unity.

(2) The product of the two f-factors at each split is equal to unity.

(3) Equal n-values occur at each split, but unequal n-values may be associated with the same stress at different temperature levels. For example, in the above tree relative humidity shows endurance exponents of 1.46 and 0.64 at the low and high levels of the thermal stress, respectively.

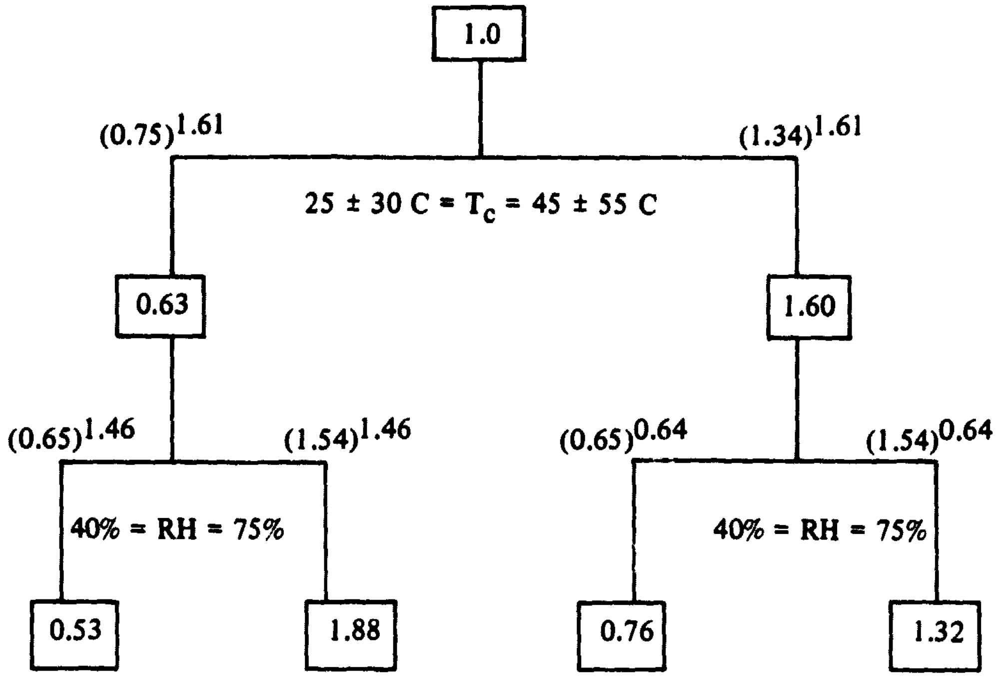

Applicability of the Model

The preceding results suggest that this rather simple, but general, model will be useful for the design and analysis of accelerated aging tests. The model appears to be consistent with an assumed special case of the Eyring relation and also provides further useful interpretations of the hierarchical trees previously proposed for generating cost-effective experimental designs. Perhaps the most important development is the manner in which the endurance exponents, made explicit by the special case of the Eyring relation, can be easily estimated from the hierarchical tree. Because these exponents are useful for the estimation of service life, it is clear that this approach has considerable promise as a general method for the design and analysis of accelerated life-prediction tests.

REFERENCES

(1) Gaines, G. B., Thomas, R. E., et al., "Methodology for Designing Accelerated Aging Tests for Predicting Life of Photovoltaic Arrays", Battelle-Columbus Final Report, ERDA/JPL-954328-77/1, 1977.

(2) Thomas, R. E., Gaines, G. B., "Methodology for Designing Accelerated Aging Tests for Predicting Life of Photovoltaic Arrays", DOE/NBS Workshop on Stability of Thin Film Solar Cells and Materials, Washington, D.C., May 1-3, 1978.

(3) Thomas, R. E., Gaines, G. B., "Procedure for Developing Experimental Designs for Accelerated Tests for Service-Life Predictions", Thirteenth Photovoltaic Specialists Conference – 1978, Washington, D.C., June 5-8, 1978.

(4) Simoni, L., "A New Approach to the Voltage-Endurance Test in Electrical Insulation", IEEE Transactions on Electrical Insulation, EI-8, pp 76-86, 1973.

(5) Mann, N. R., Schafer, R. E., Singpurwalla, N. D., *Methods for Statistical Analysis of Reliability and Life Data,* John Wiley & Sons, Inc., New York, 1974.

(6) Thomas, R. E., Gorton, H. C., "Research Towards a Physics of Aging of Electronic Component Parts", Proceedings of Second Symposium on the Physics of Failure, 1964.

(7) Hatch, B. D., Endicott, H. S., Sohmer, R. G., "Application of the Eyring Model to Capacitor Aging Data", Technical Information Series, No. R62SD169, Missile and Space Division, General Electric.

FUTURE WORK

In the work so far, potential degradation modes of the Mead modules have been postulated, judgments have been made as to the stresses which accelerate the degradation of the power output, composite severity ratings have been formulated for combining several degradation modes, and a start has been made on the formulation of test groupings (Table 3) which represent experimental and cost realities and which at the same time cover the expected degradation modes. The next major task is to devise specific tests within each test group and among groups so that acceptable statistical validity is realized in life prediction at an acceptable cost.

Once the statistical design is satisfied, the effort will turn toward a calculation of the number distribution of test specimens among the specific test conditions, in the manner prescribed in the referenced Study-4 report[1].

Finally, the measurement schedule, the instrumentation, and general data formats will be specified.

APPENDIX A

HIERARCHICAL TREES REPRESENTING THE MAIN EFFECTS AND INTERACTIONS OF ENVIRONMENTAL STRESSES ON INDIVIDUAL DEGRADATION MODES

APPENDIX A

HIERARCHICAL TREES REPRESENTING THE MAIN EFFECTS AND INTERACTIONS OF ENVIRONMENTAL STRESSES ON INDIVIDUAL DEGRADATION MODES

As noted in the main text, hierarchical trees have been developed for each individual degradation mode. They are presented in this appendix. "H" and "L" used on the hierarchical trees that follow denote respectively, the high and low levels of the stress in question. It is to be noted that a high level of a stress need not necessarily represent a larger degradation rate than a lower level of stress. One can hypothesize situations in which an extremely low temperature or relative humidity might be more severe than higher levels of the same stresses.

On a tree, the horizontal distance separating the high and low levels of a stress reflect the sensitivity to that stress of the phenomenon (degradation mechanism) in question.

In general, there is no quantitative significance to the vertical level of stresses in a tree. In the trees in Figures A-1 through A-11, the stresses in the second, third, and lower levels have been vertically positioned as shown in order to facilitate visual interpretation.

The stresses in the lowest level have been marked only with + (=H) and x (= low) to avoid unnecessary clutter.

The stress severity ratings in this report have all been normalized to 100.

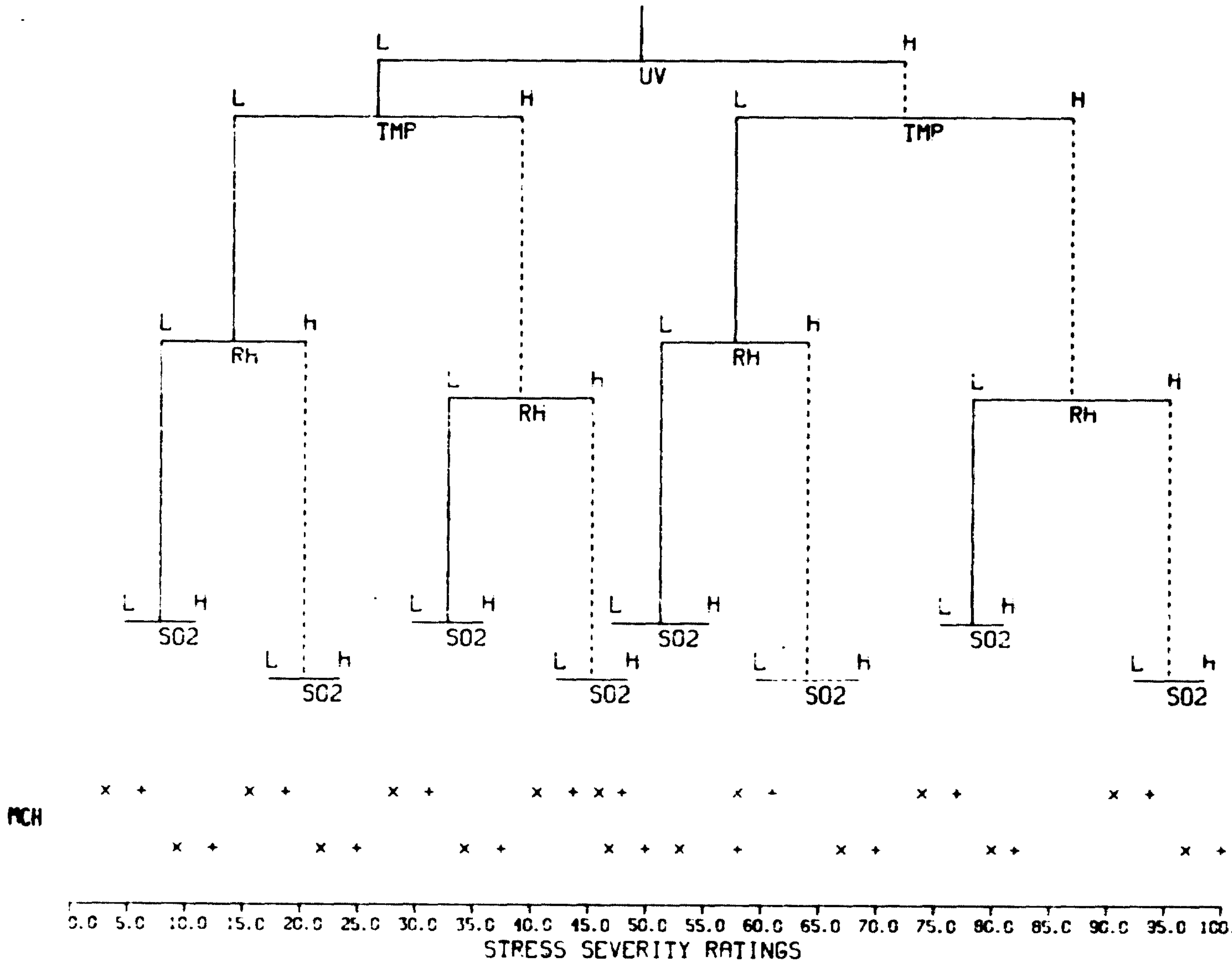

FIGURE A-1. A HIERARCHICAL TREE ASSOCIATED WITH DECREASE IN TRANSMISSION – CONSTANT TEMPERATURE

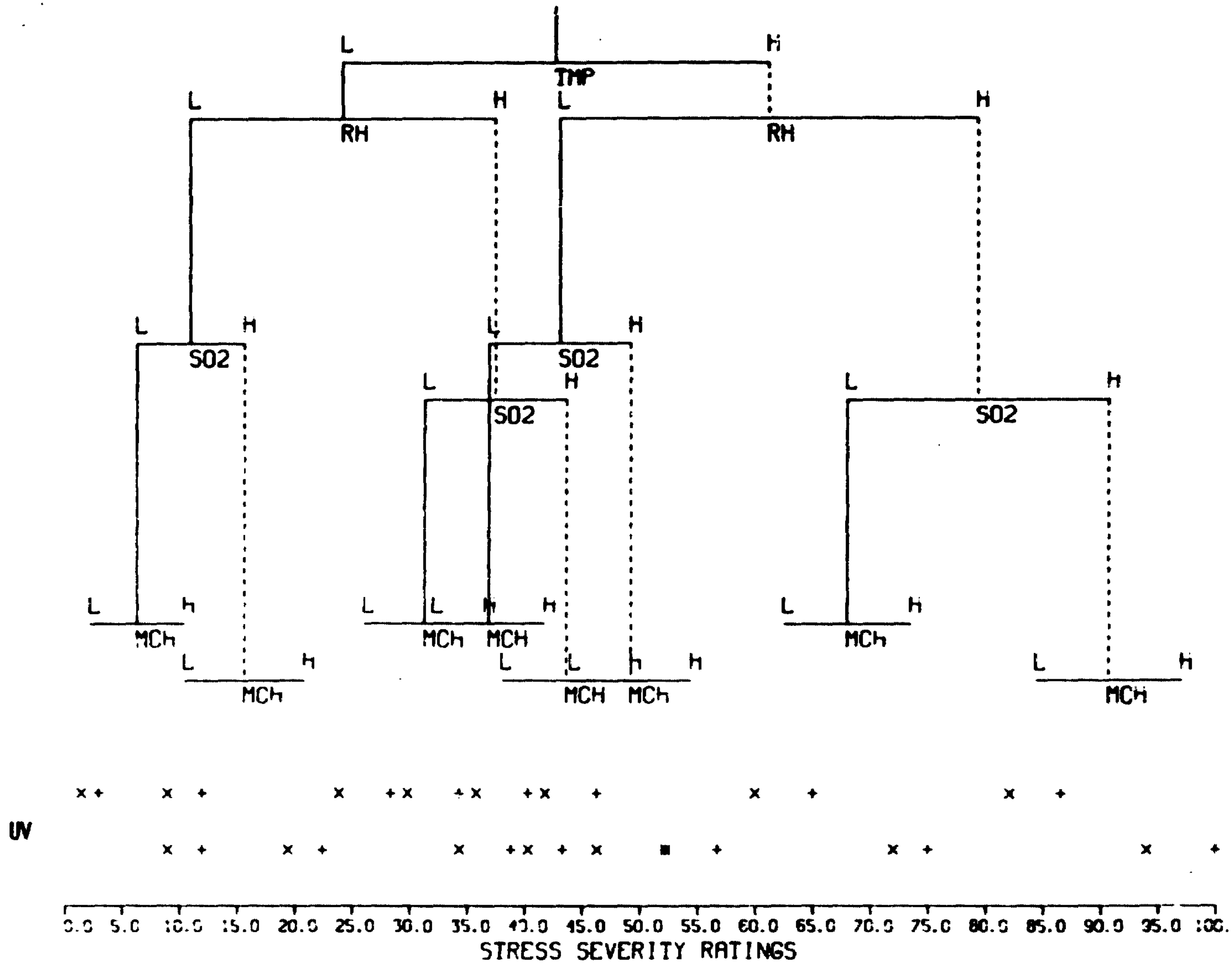

FIGURE A-2. A HIERARCHICAL TREE ASSOCIATED WITH INCREASE IN CELL SERIES RESISTANCE – CONSTANT TEMPERATURE

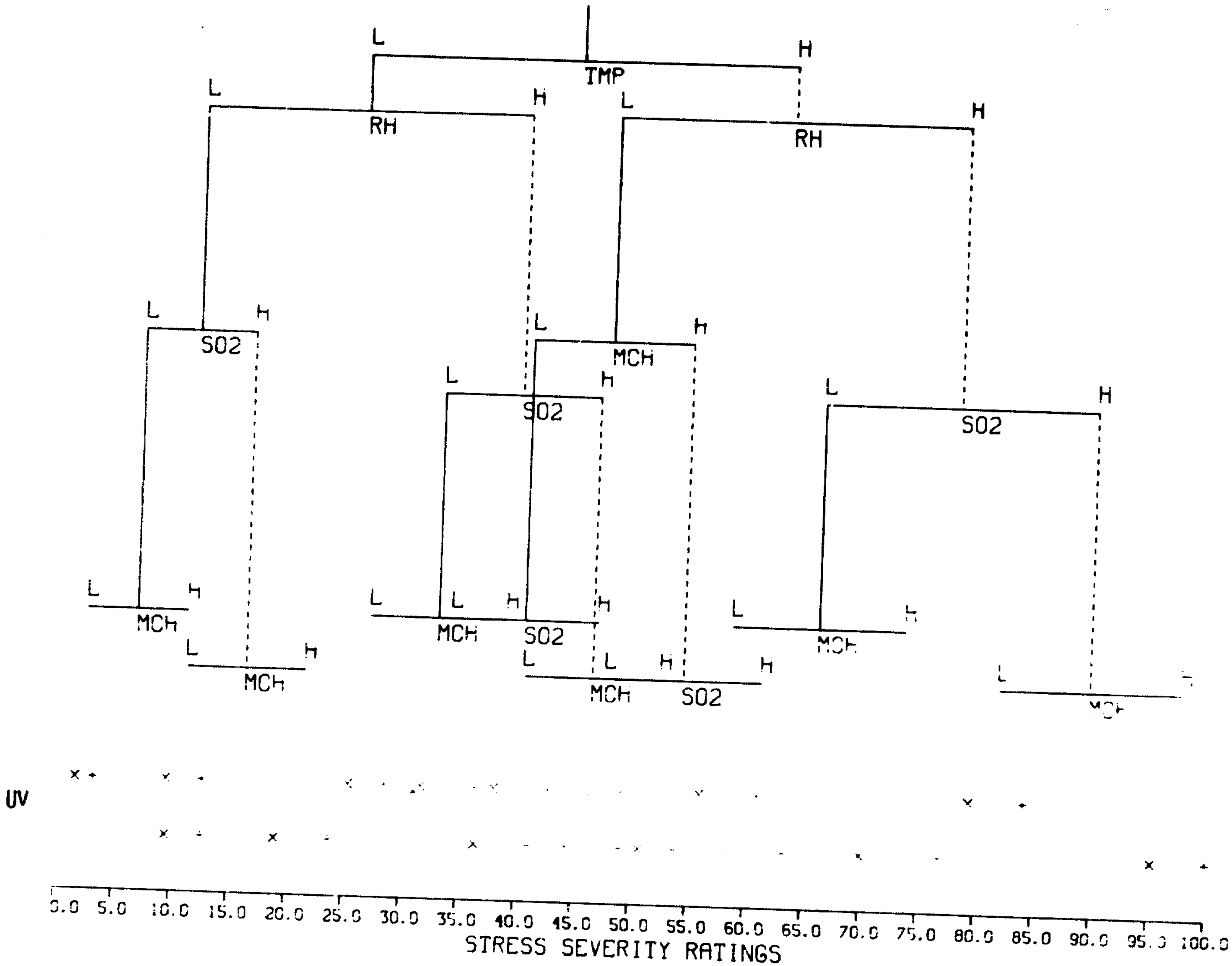

FIGURE A-3. A HIERARCHICAL TREE ASSOCIATED WITH INCREASE IN CELL SERIES RESISTANCE – CYCLIC TEMPERATURE

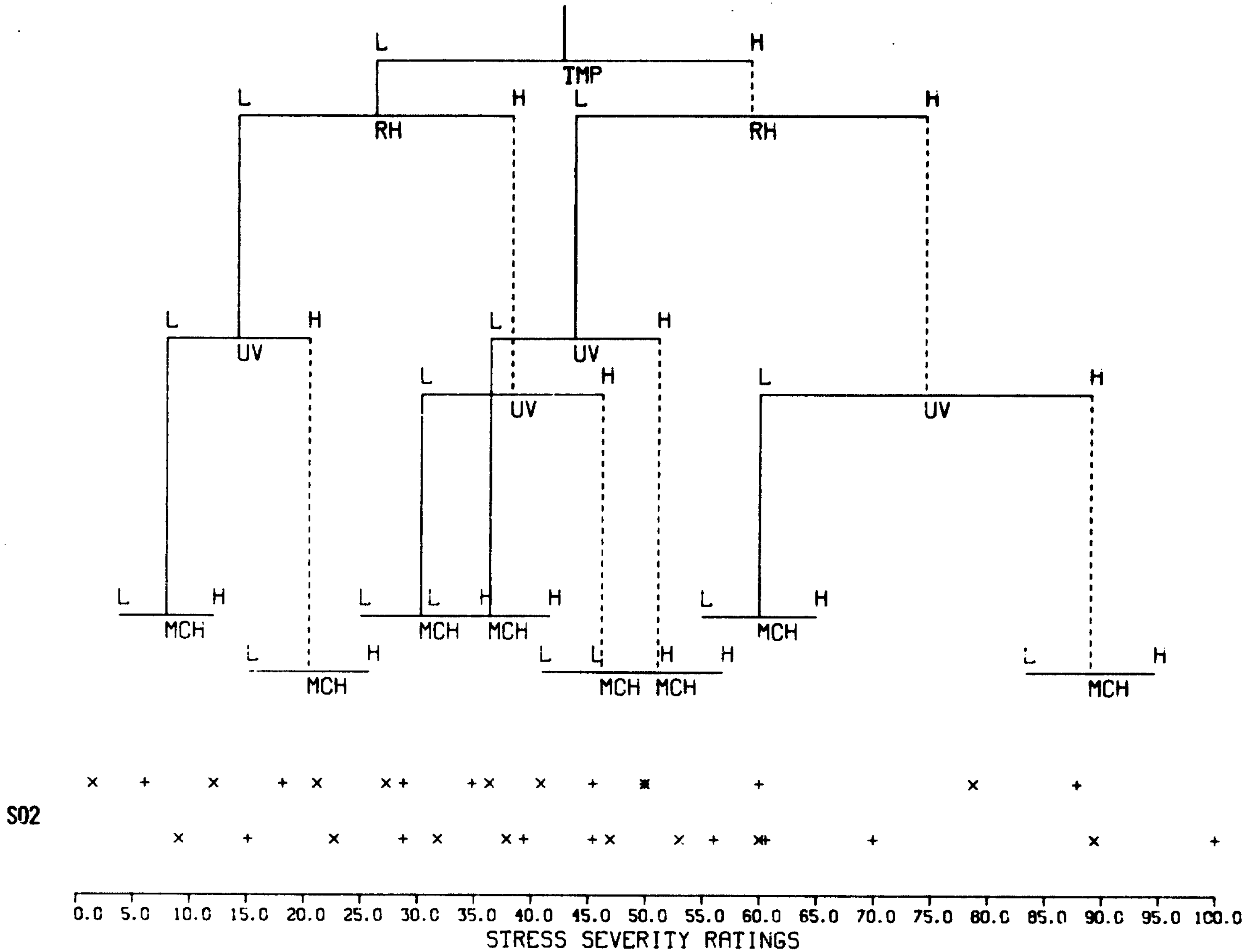

FIGURE A-4. A HIERARCHICAL TREE ASSOCIATED WITH DELAMINATION – CONSTANT TEMPERATURE

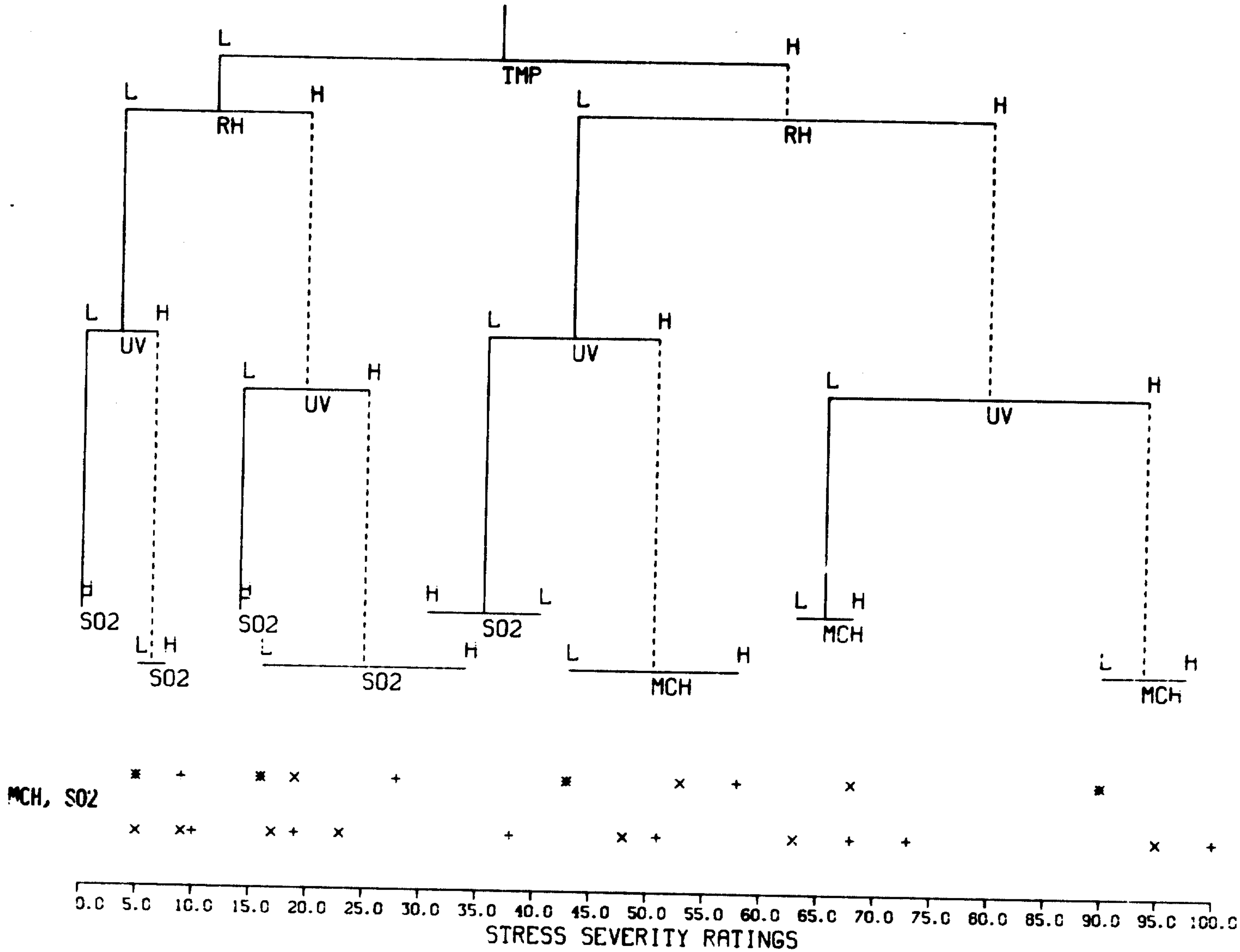

FIGURE A-5. A HIERARCHICAL TREE ASSOCIATED WITH DELAMINATION – CYCLIC TEMPERATURE

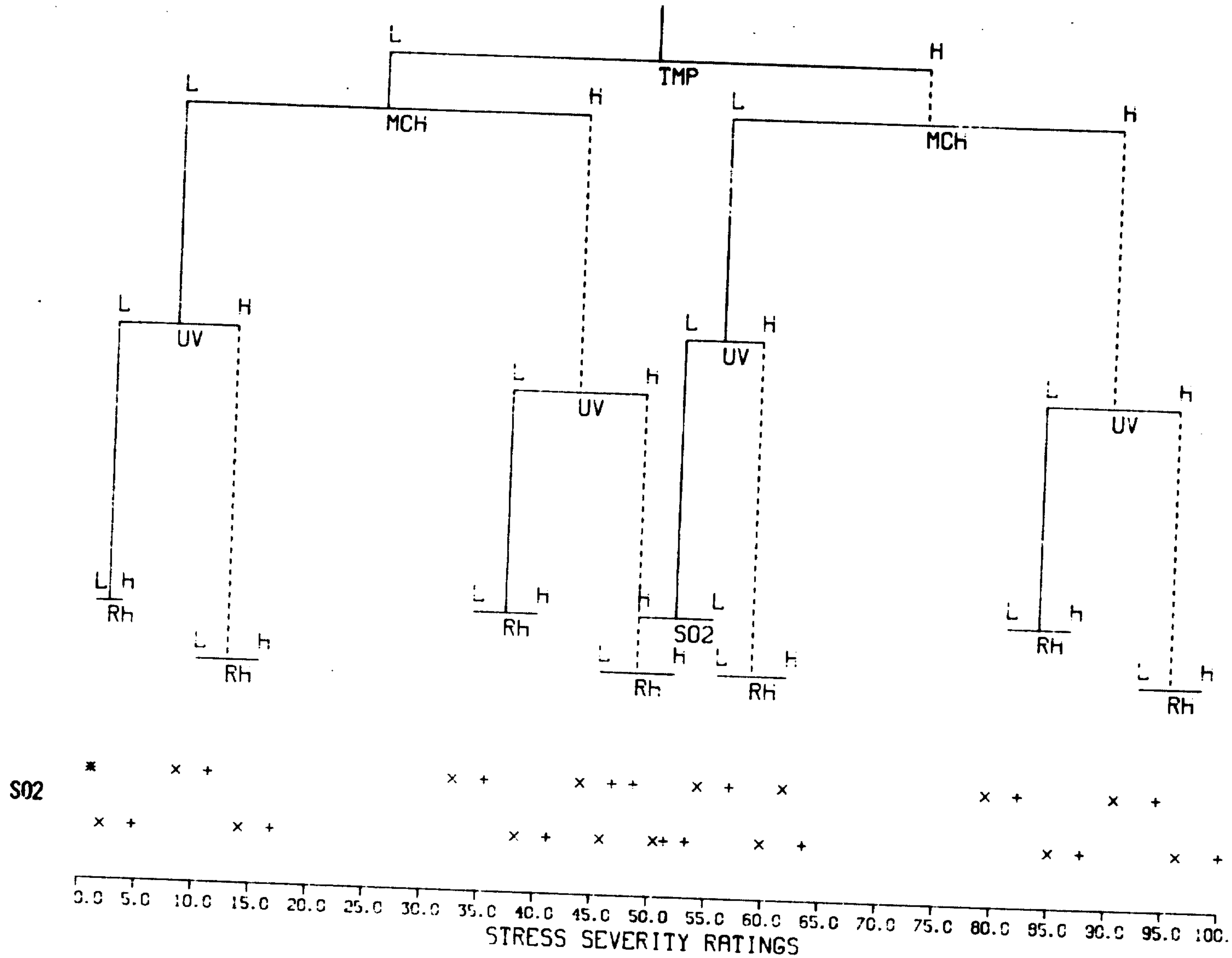

FIGURE A-6. A HIERARCHICAL TREE ASSOCIATED WITH CELL CRACKING – CONSTANT TEMPERATURE

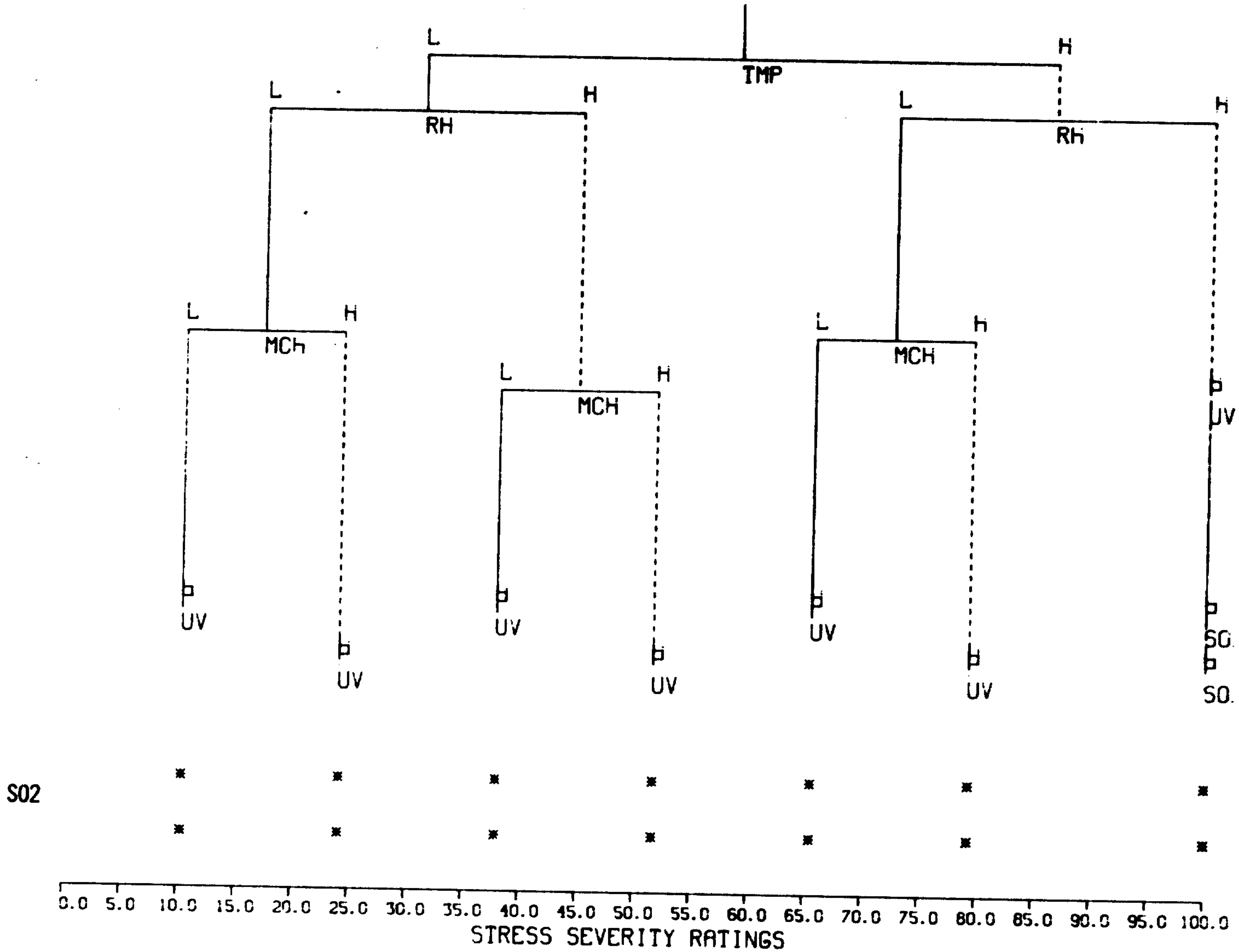

FIGURE A-7. A HIERARCHICAL TREE ASSOCIATED WITH CELL CRACKING – CYCLIC TEMPERATURE

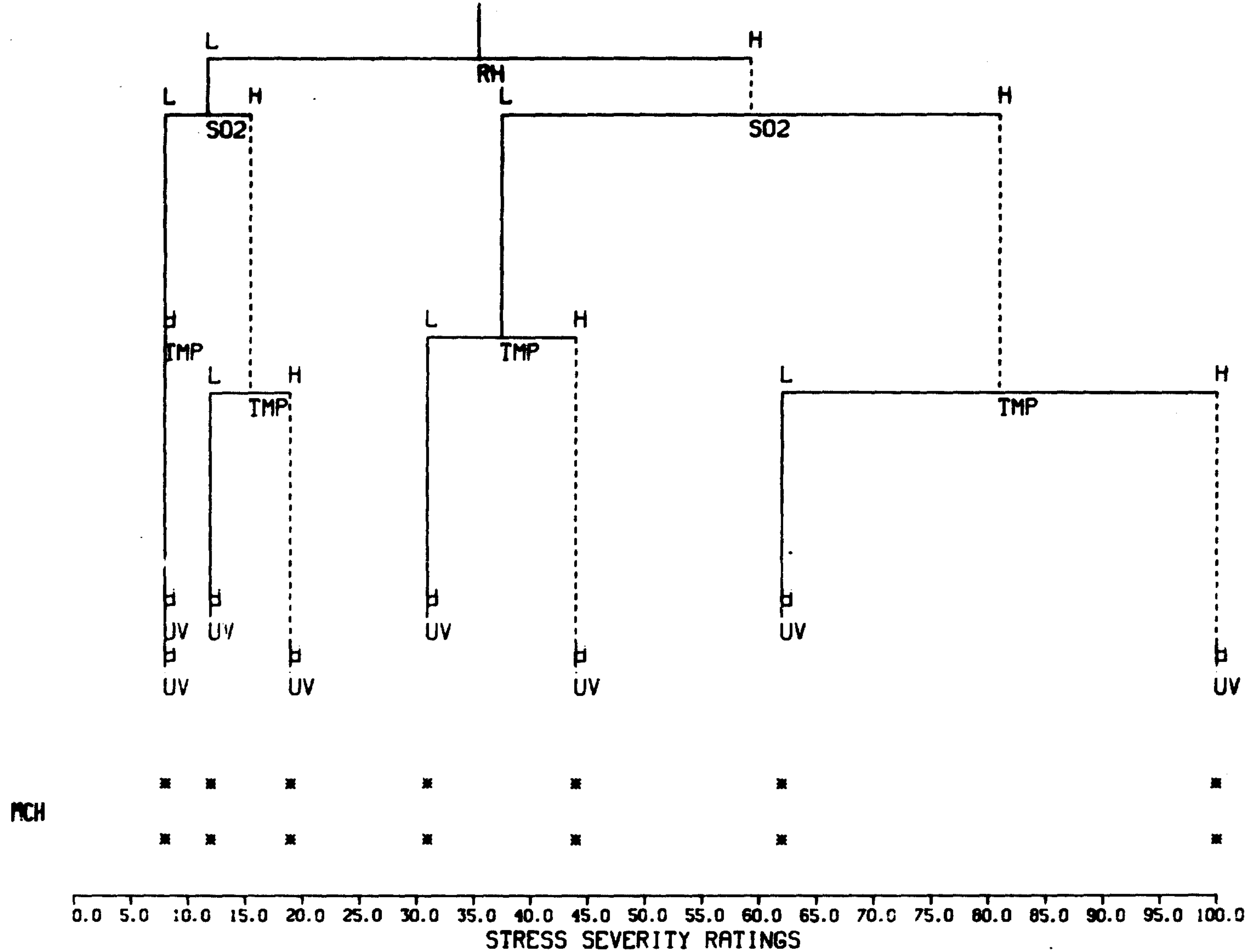

FIGURE A-8. A HIERARCHICAL TREE ASSOCIATED WITH INTERCONNECT CORROSION – CONSTANT TEMPERATURE

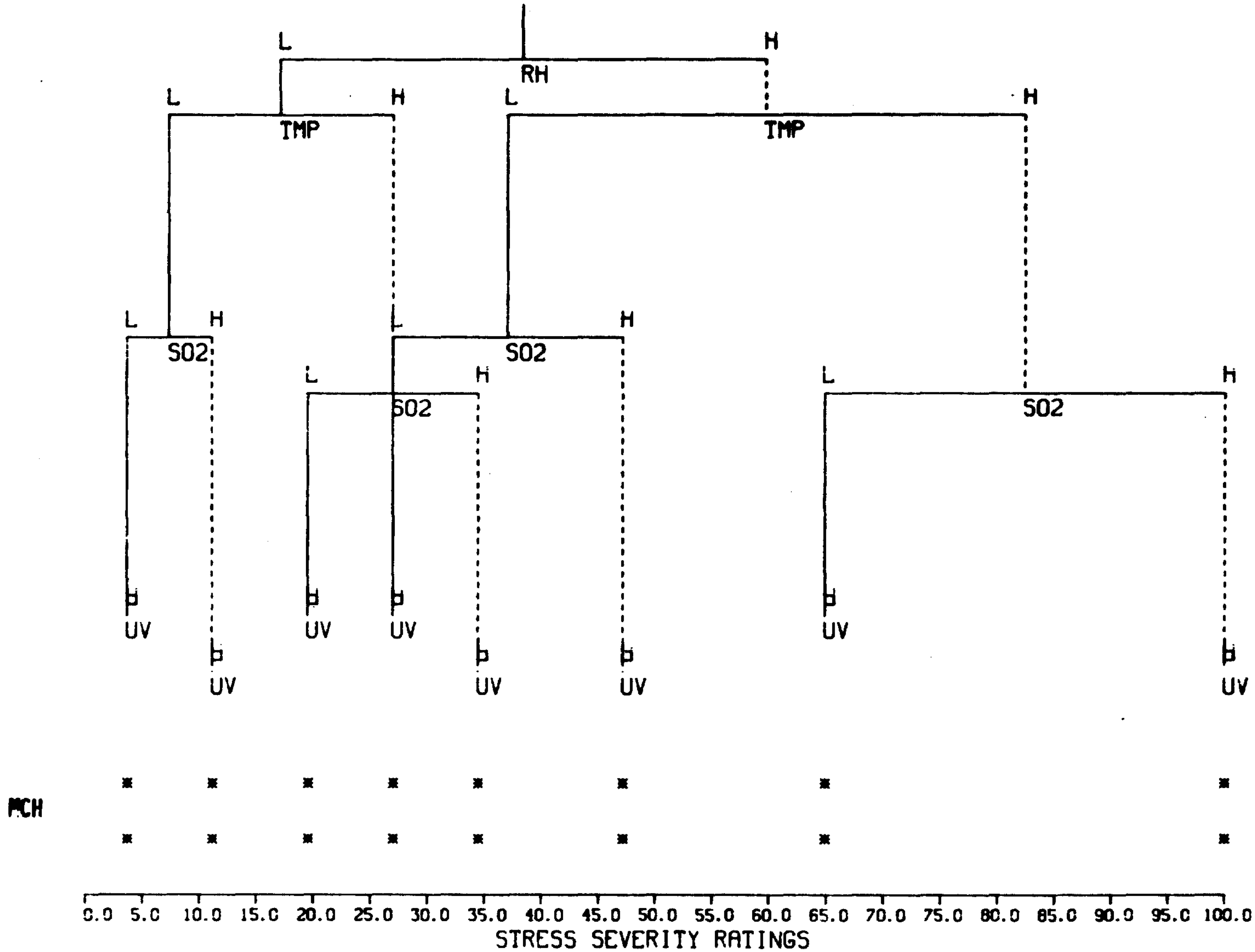

FIGURE A-9. A HIERARCHICAL TREE ASSOCIATED WITH INTERCONNECT CORROSION – CYCLIC TEMPERATURE

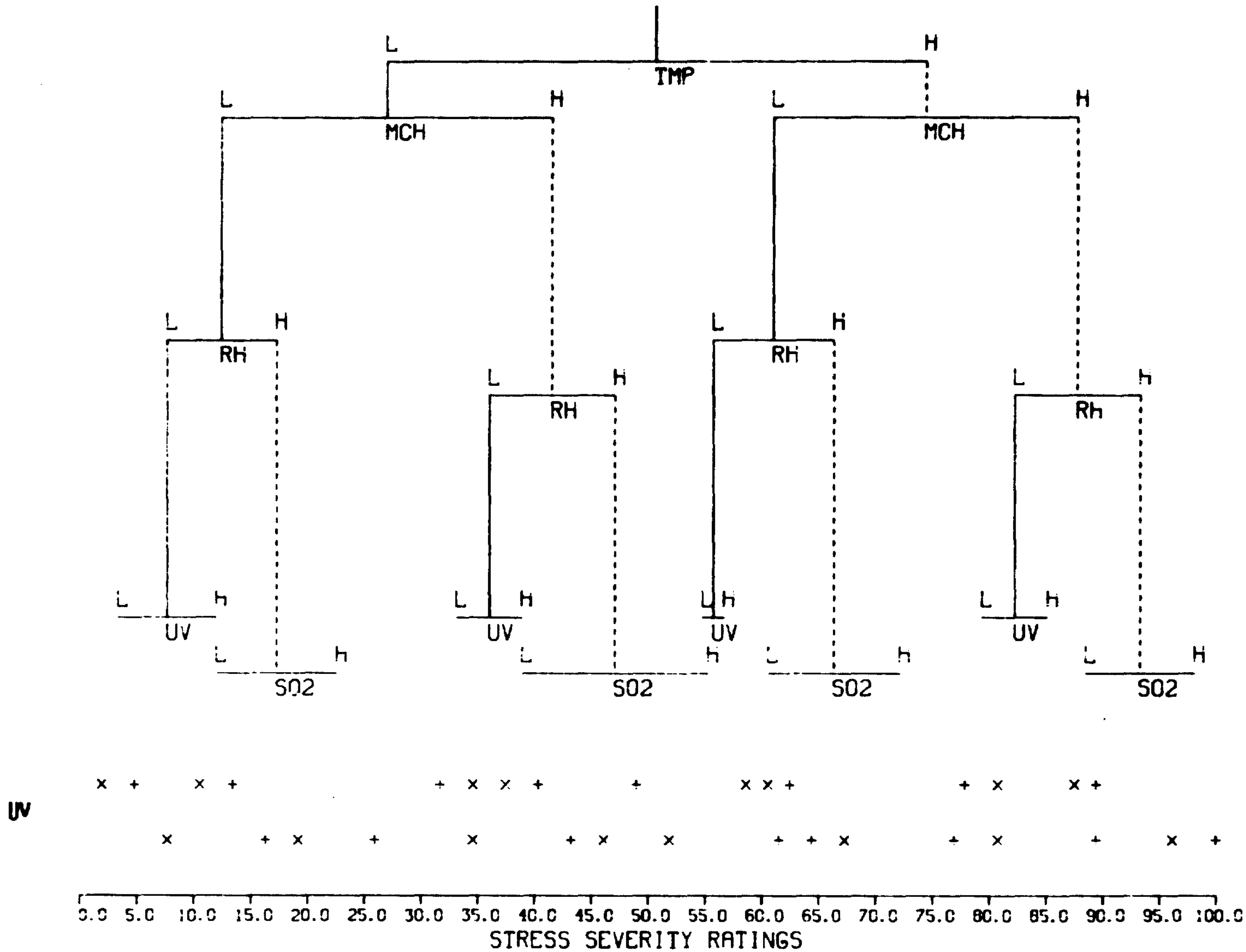

FIGURE A-10. A HIERARCHICAL TREE ASSOCIATED WITH INTERCONNECT BREAKAGE – CONSTANT TEMPERATURE

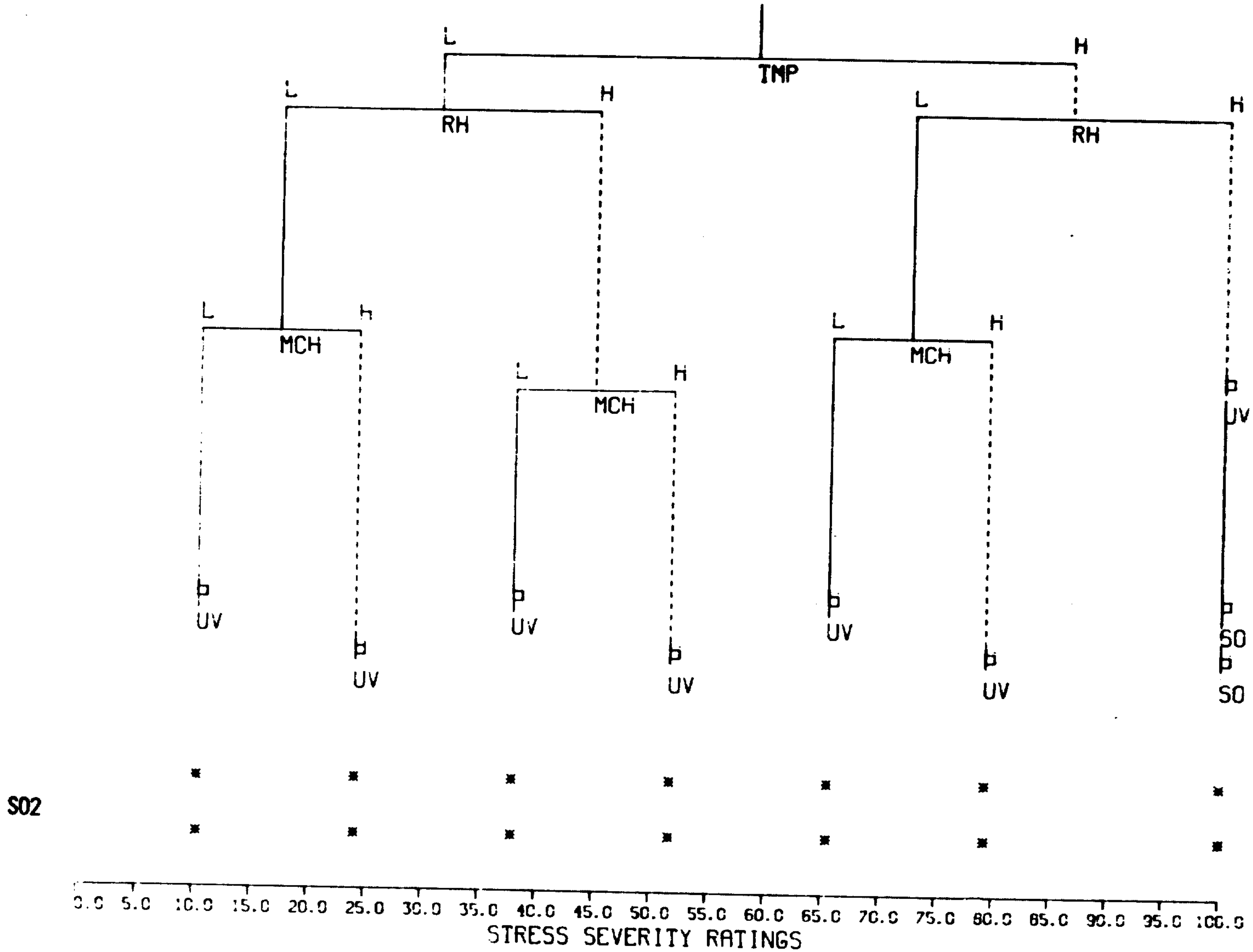

FIGURE A-11. A HIERARCHICAL TREE ASSOCIATED WITH INTERCONNECT BREAKAGE – CYCLIC TEMPERATURE